A NEW VOLTAGE STABILITY INDEX FOR PREDICTING VOLTAGE COLLAPSE IN ELECTRICAL POWER SYSTEM NETWORKS

By

SAMUEL Isaac Adekunle

CUGP070183

M Eng. (Power and Machine) (Kano)

JANUARY, 2017

A NEW VOLTAGE STABILITY INDEX FOR PREDICTING VOLTAGE COLLAPSE IN ELECTRICAL POWER SYSTEM NETWORKS

By

SAMUEL Isaac Adekunle

M Eng. (Power and Machine) (Kano)

Matric No: CUGP070183

A THESIS SUBMITTED TO THE SCHOOL OF POST GRADUATE STUDIES OF COVENANT UNIVERSITY, OTA, OGUN STATE NIGERIA

IN PARTIAL FULFILMENT OF THE REQUIREMENTS FOR THE AWARD OF DOCTOR OF PHILOSOPHY (Ph.D) DEGREE IN ELECTRICAL POWER AND MACHINES, IN THE DEPARTMENT OF ELECTRICAL AND INFORMATION ENGINEERING, COLLEGE OF ENGINEERING, COVENANT UNIVERSITY, OTA, NIGERIA.

JANUARY, 2017

ACCEPTANCE

This is to attest that this thesis is accepted in partial fulfilment of the requirement for the award of the degree of the **Doctor of Philosophy (Ph.D) Degree in Electrical Power and Machine** in the Department of **Electrical and Information Engineering**, College of Engineering, Covenant University, Ota, Nigeria.

Philip John Ainwkhai	…………………
Secretary, School of Postgraduate Studies	Signature & Date
Prof. Samuel Wara	…………….……
Dean, School of Postgraduate Studies	Signature & Date

DECLARATION

I, **SAMUEL Isaac Adekunle** (CUGP070183) declare that this research was carried out by me under the supervision of Prof. James Katende of College of Engineering and Technology, Botswana International University of Engineering and Technology, Botswana and Prof. C. O. A. Awosope of the Department of Electrical and Information Engineering, College of Engineering, Covenant University, Ota. I attest that the thesis has not been presented either wholly or partly for the award of any degree elsewhere. All sources of data and scholarly information used in this thesis are duly acknowledged.

SAMUEL Isaac Adekunle ....

Signature & Date

CERTIFICATION

We certify that the thesis titled "A NEW VOLTAGE STABILITY INDEX FOR PREDICTING VOLTAGE COLLAPSE IN ELECTRICAL POWER SYSTEM NETWORKS" is an original work carried out by SAMUEL Isaac Adekunle, (CUGP07018), in the Department of Electrical and Information Engineering, College of Engineering, Covenant University, Ota, Ogun State, Nigeria, under the supervision of Prof. James Katende and Prof. C. O. A. Awosope. We have examined and found the work acceptable for the award of degree of Doctor of Philosophy in Electrical and Electronics Engineering (Electrical Power and Machines).

Supervisor:

Prof. James Katende …………………..

Signature & Date

Co-Supervisor

Prof. C.O.A Awosope …………………..

Signature & Date

Head of Department

Dr. Victor O. Matthews ………………….

Signature & Date

External Examiner

Prof. Michael O. Omoigui ………………….

Signature & Date

Dean, School of Postgraduate Studies

Prof. Samuel Wara ………………….

Signature & Date

DEDICATION

This project is dedicated to my beloved wife, Comfort O. Samuel and my children, Israel Oluwatobiloba Samuel, Miss Lois Toluwani Samuel, Timothy Oluwatosin Samuel and Titus Oluwatimileyin Samuel.

And to the blessed memory of my father, His Royal Highness, Oba Ayodele Samuel Agunbole, the Olutade of Itedo-Isanlu, my beloved mother, Deaconess Rachel Mini Agunbole and my Father-in-law, Pa Christopher Babatunde Ogagun. May their souls continue to rest in peace. Amen.

ACKNOWLEDGEMENTS

Psalms 115.1: “Not to us, LORD, not to us, but to your name be given glory on account of your gracious love and faithfulness” (ISV). Thanks are due to the Almighty God through Jesus Christ for His inspiration, guidance, protection and provision for the successful completion of this Ph.D programme.

I sincerely appreciate the Management of Covenant University under the leadership of Prof. A.A.A. Atayero, the Vice-Chancellor and Prof. C.K. Ayo, the immediate past Vice-Chancellor, for providing a highly conducive environment for research and learning. I am also indebted to the visionally-extraordinaire and Chancellor of Covenant University, Dr. David Oyedepo.

My profound gratitude goes to my supervisor, Professor James Katende, who gave me all the necessary assistance to ensure that this thesis is completed successfully. I am also indebted to him, as well as his wife, Mrs. O. A. James-Katende and their children, for being a wonderful and delightful host during my research leave at the Botswana International University of Science and Technology, Palapye, Botswana. Thanks are due to my co-supervisor, Professor C. O. A. Awosope, a father and great motivator who accepted to co-supervise this work in the nick of time. His contributions, encouragement and support throughout this research work are inestimable and highly treasured, thank you sir. Much appreciation to my point man at the National Control Centre, Osogbo, Engr. Eric Hampashi for his kind gesture during data acquisition.

I sincerely appreciate the current Head of Department, Dr. Victor O. Matthews for his support and encouragements. The immediate past Head of Department, Dr. F. Idachaba for facilitation of my research leave even when it seemed impossible. I also appreciate all faculty and staff of the Department for their encouragement and moral support. I say a very big thank you to you all.

Proverbs 18.24 "…there is a friend that sticketh closer than a brother" (KJV), Dr. Ayokunle Awelewa, thank you for your words of encouragement, moral and spiritual support and relevant contributions to this work. I specially acknowledge my academic mother and mentor, Prof. Alaba Simpson-Badejo; my brothers, sister and brother in-law, Barr. 'Yomi Omoyele, for all their support. Thanks are due to the Ogaguns, the Olokodes and the Ogunjimis for their support.

My heartfelt appreciation goes to Pastor Bunmi and Dapo Ajegunmo, and entire set of ministers at Calvary Life Assembly, Yaba, Lagos for their prayers and support. I am greatly indebted to Pastor Rupo Awelewa for his uncommon support. Thank you so much.

May God bless every one that has contributed in one way or the other to the success of this program in Jesus'name. It's my sincere prayer for the full expression of Philip. 4.19 in the lives of everyone that God used to bring this dream to reality. Amen.

TABLE OF CONTENTS

LIST OF FIGURES

LIST OF TABLES

LIST OF SYMBOLS AND ABBREVIATIONS

CIGRE:	International Council on Large Electric Systems
DAE:	Differential and Algebraic Equations
D_{base} :	Index Base value
D_{used} :	Index Value used
E_{abs} :	Absolute error
E_{rel} :	Relative error
FVSI:	Fast Voltage Stability Index
GDP:	Gross Domestic Product
HVDC:	High Voltage Direct Current
IEEE:	Institute of Electrical and Electronics Engineers.
J:	Jacobian matrix
Lmn:	Line Stability Index
LPQ:	Line Stability Factor
LVSI:	Line Voltage Stability Index
NERC:	Nigerian Electricity Regulatory Commission
NLSI:	New Line Stability Index
NNG:	Nigerian National Grid
NR:	Newton-Raphson method
P_{gen}:	Generated active power
P_i :	Active power of the *ith* bus
P_{load}:	Real power delivered to load
P_{max} :	Maximum Active Power
PMU:	Phasor Measurement Unit
P_s , P_r :	Real power at sending bus ‘s’ and the real power at receiving bus ‘r’
PSN:	Power System Network
pu:	Per unit
P-V Curve:	Active Power-Voltage curve
Q_{gen}:	Generated reactive power

Q_i :	Reactive power of the *ith* bus
Q_{load}:	Reactive power delivered to load
Q_s , Q_r :	Reactive powers at the sending and Receiving buses 's' and bus 'r' respectively.
Q-V Curve:	Reactive Power- Voltage curve
R:	Line resistance
S:	Apparent power
S_{load}:	Apparent power delivered to load
S_s , S_r :	apparent Power at the sending bus 's' and the apparent power at the receiving bus 'r'.
TCN:	Transmission Company of Nigeria
VCPI:	Voltage Collapse Point Indicator
V_i .:	Voltage magnitude of the *ith* bus
V_m :	Magnitude of voltage at bus
V_s , V_r :	Sending voltage and Receiving voltage.
X:	Line reactance
Y:	Admittance matrix
Z:	Line Impedance
σ:	Switching function
θ:	Transmission line angle
% E :	Percent error
δ:	Difference between δ_s and δ_r
δ_s , δ_r :	Voltage angles of the sending and the receiving buses 's' and bus 'r' respectively.
ΔP:	Difference between specified and calculated values of real power
ΔQ:	Difference between specified and calculated values of reactive power
ΔV:	Difference between specified and calculated values of voltage magnitude.
$\Delta\delta$:	Difference between specified and calculated values of voltage angle

ABSTRACT

Power system voltage instability often results in voltage collapse and/or system blackout which is a source of concern for power network operators and consumers. This work proposes a new line stability index that is suitable for investigating the voltage stability condition of Power System Networks (PSNs). This index, which is called the New Line Stability Index-1 (NLSI_1), is derived from first principles and shown to incorporate the Line Stability Index (Lmn) and the Fast Voltage Stability Index (FVSI), with an associated switching logic based on the voltage angle difference since it can indicate the incidence of voltage collapse. The NLSI_1 aims at improving the accuracy and speed of identifying the weakest bus associated critical lines with respect to a bus for purposes of optimally placing compensation devices as well as investigating the effect of increasing reactive power loading on the PSN. The developed index (NLSI_1) was tested on the IEEE 14-bus system and the present 28-bus, 330-kV Nigeria National Grid (NNG) using a program coded in the MATLAB environment. The three indices were then simulated for the base case and the contingency – variation of the reactive loads in the network. For the base case, the IEEE 14-bus test system was stable with all the three indices approximately equal and < 1 for all the lines. Contingency simulations were carried out revealing that bus 14 ranks as the weakest bus of the system, with the smallest reactive load of 74.6 MVAr among the load buses. The values of the indices, Lmn, FVSI and NSLI_1 are approximately equal for the IEEE 14-bus system thereby validating the efficacy of the new line stability index-1 (NLSI_1). For the NNG system, the power flow solution showed that the voltage profiles for load buses 9, 13,14,16,19 and 22 (Kano, Gombe, New Haven, Jos, Ayede and Onitsha, respectively) have voltage magnitudes 0.932, 0.905, 0.949, 0.844. 0.93, and 0.818 p.u, respectively against the voltage criterion of 0.95 p.u. These low voltages are indication that the network buses are prone to voltage instability. The base case of the NNG simulation values for all three indices (Lmn, FVSI and NLSI_1) were less than unity (<1) for all the lines. Hence, in the base case, the NNG is stable. It was observed that the three indices' values are almost equal (the largest difference being 0.004) which further validates the newly derived index, NLSI_1. In the simulation of the contingency scenario, load bus 16 (Gombe) was observed to be the weakest since it has the smallest maximum permissible reactive load of 139.5 MVAr with the stability indices, Lmn=0.95474, FVSI=1.00942 and NLSI_1=1.00942 indicating incipient instability of the bus. The new line stability index-1 (NLSI_1) combines the accuracy of the Lmn index and the fastness of the FVSI index for an improved voltage stability prediction.

Keywords: Voltage stability, Voltage collapse, Voltage stability indices, Weakest bus, Power system networks, NNG, MATLAB, Critical line.

CHAPTER ONE
INTRODUCTION

1.1 Background

The voltage stability of a power system network (PSN) has, over the past two decades, become a critical concern with respect to system design, planning, and operation. This is in view of the fact that globally, PSNs have undergone major developments culminating in the unbundling of vertically integrated entities to operate under different power utility companies. Consequently, driven by market forces and profitability, the new power utility companies operate the power transmission corridors close to voltage stability limits (Arya, 2006; Samuel *et al,* 2014). This has led to several violations of overall system stability limits resulting in PSN voltage collapse incidences around the world with high cost implications to both utilities and consumers (Goh *et al,* 2015; Hasani, and Parniani, 2005). A PSN must therefore be monitored so as to predict and create an alert of possible occurrence of voltage collapse incidences.

In recent years, following the unbundling and privatization of power system networks, their management has become increasingly more challenging in the face of systems being operated close to their security limits; with restricted expansion due to economic and environmental constraints and increasingly longer transmission lines. Privatization has also meant a reduction in manpower available for system supervision and operation. The number of system blackouts in the past decade attests to the fact that work still needs to be done to tackle the problem of voltage instability and the resultant voltage collapse.

The function of a PSN is to generate and transmit power to load centres at specified voltage and frequency levels. Statutory limits exist for system voltage and frequency variations about base levels (Samuel *et al.,* 2014 (a)). Today's PSNs are said to be weak, heavily loaded and highly prone to voltage instability. This is due to increasing load demand resulting from population growth and industrialization, as well as environmental and economic factors. These hamper the construction of new transmission lines and generating stations to cater for increasing demand (Reddy and Manohar, 2012 ; Hasani and Parniani, 2005).

Voltage stability as defined by P. Kundur is "the ability of a power system to maintain steady and acceptable voltages at all buses in the system at normal operating conditions and after being subjected to a disturbance" (Kundur, 1994). It is desired that the power system remains in an equilibrium state under normal conditions and it is expected to react to restore the status of the system to acceptable conditions after a disturbance, i.e. the voltage after a disturbance is restored to a value close to the pre-disturbance situation.

A PSN is said to enter a state of voltage instability when a disturbance causes a gradual and uncontrollable decline in voltage (Sarat *et al.,* 2012). The causes of voltage instability are contingencies (line or generator outage due to faults), sudden increase in load, external factors, or improper operation of voltage control devices. More importantly, voltage instability can surface where there is a mismatch between supply and demand of reactive power, that is, inability of the system to meet the reactive power requirements. Unmitigated voltage instability caused by excessive load on a PSN leads to a decline in system voltage and ultimately a voltage collapse resulting in a partial or total system blackout. This has severe consequence on system security and it jeopardizes the essential service of delivering uninterrupted and reliable power supply to customers (Veleba and Nestorovic, 2013).

In real-time PSN operation, it is very important that voltage stability analysis is performed and a stability index used to monitor the voltage stability proximity to collapse and to predict the imminent danger of collapse early enough. This is with a view to alerting system operators to take neccessary action to avert a voltage collapse thereby, making the PSN more secure and reliable. Figure 1.1, shows the progress of a voltage collapse phenomenon.

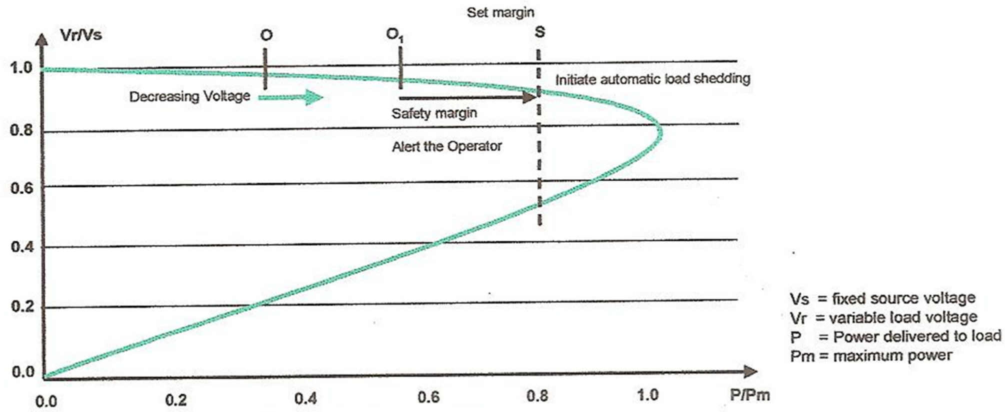

Figure 1.1: Progress of a voltage collapse event (Samuel et al., 2014 (a))

The system voltage decreases slowly as the demand increases until a critical point is reached. At this point, any slight increase in demand will give rise to a large decrease in voltage, until the demand can no longer be met, and eventually leads to voltage collapse on the system (Samuel *et al,* 2014 (a)). Consequently this experience on PSN creates a need to develop and derive reliable voltage stability indices for PSN assessment.

1.2 Statement of the Problem

Voltage collapse in a PSN is an undesirable phenomenon that occurs due to voltage instability. Its occurrence is not frequent in developed countries despite their large and complex networks (though it still poses a threat to continuity of supply to consumers) but it occurs more frequently on the power networks of most developing countries including Nigeria.

Voltage collapses are highly catastrophic anytime they occur. Some instances of power system collapse experienced in recent times across the world have been reported in Kundur, (1994), Taylor, (1994), Kundur *et al.,* (2004), Ali, (2005), Anyanwu, (2005), and Sunday, (2009).

In a developing country like Nigeria, the national grid experiences high rate of voltage collapse leading to either partial or total system collapse (blackout), which greatly impairs socio-economic development and industrialization. This high rate of system collapse is attributed to the fact that the Nigerian National Grid (NNG) is weak and highly stressed, with long and radial transmission lines, hence lacking flexibility (Ali, 2005; Anyanwu, 2005; Amoda, 2007; Sunday, 2009 and Samuel, *et al.,* 2014 (a)). When a voltage collapse occurs, restoration of power may take a long time.

The present study seeks to develop a voltage stability index suitable for PSN monitoring for purposes of predicting incipient system voltage instability and the possibility of a voltage collapse event. The study will also identify the weak bus and critical lines with respect to a bus in order to determine the optimum deployment of the compensation devices and voltage collapse relays within the PSN.

1.3 Aim and Objectives of the Study

The primary aim of this study is to assess and predict voltage collapse in power system networks.

The objectives to achieve the aim are as follows:

(i) Develop a new voltage stability index suitable for predicting voltage collapse of power system networks.

(ii) Investigating the proposed voltage stability index in MATLAB environment and its application to the simulation of:

   a) the IEEE 14-bus network and comparing it with the existing stability indices for validation of the proposed voltage stability index.

   b) a practical system: the NNG 28-bus system and comparing it with the existing stability indices with a view to determining closeness to voltage collapse, maximum loadability, the critical line, and the ranking of vulnerable buses.

(iii) Apply Newton-Raphson method of power-flow analysis to analyze the IEEE 14-bus power system and the NNG 28-bus, 330-kV power system in order to generate the data required to calculate the voltage stability indices.

(iv) Simulate the voltage stability using MATLAB, R2012a (7.14.0739) 32-bit (win32) environment for the base case and contingencies using the data generated from the power flow solution.

1.4 Justification for the Research

Today's power system networks are being operated closer to their transmission capacity limits due to economic and environmental constraints (Ali, 2014). The major blackouts or voltage collapse incidences have been linked to voltage instability which places limitation to system operations. The inconveniences and economic cost which the voltage collapse incidences inflict on customers (both domestic and industrial) are enormous and unpleasant. In Nigeria, the resultant power outages are estimated to cost the nation the sum of $1 billion per year, i.e. 2.5% the gross domestic product (Amoda, 2007). Inadequate electricity supply has led to the closure of several industries in Nigeria. Small businesses and manufacturers are also affected by the poor performance of the utility companies (Samuel *et al.,* 2014(a)). The World Bank reported the loss of $100b in one year due to daily blackouts experienced in Nigeria (Channels TV, 2015). It further stated that these daily power outages have made investors weary of investing in the Nigerian economy (Ogbonna, 2015).

Research on voltage collapse of the Nigerian National Grid (NNG) is scanty at the moment and the available statistics shows that the rate of voltage collapse on the NNG is very high. Table1.1 shows the statistical data of both partial (p/c) and total (t/c) collapses on the NNG from January 2005 to December 2014 (Samuel *et al.,* 2014 (a)).

Table 1.1: System Collapses: 2005-2014 on the NNG

Year	2005	2006	2007	2008	2009	2010	2011	2012	2013	2014
Partial collapse (p/c)	15	10	8	16	20	32	4	8	2	4
Total collapse (t/c)	21	20	18	26	19	9	12	18	22	9
Total	36	30	26	42	39	41	16	26	24	13

Source: Samuel *et al.,* 2014 (a)

From Table 1.1, the annual rate of total collapse may be obtained empirically from:

$$\text{Annual rate of collapse} = \frac{\text{Total No.of collapse during a given period}}{\text{the given period}} \quad \ldots\ldots\ldots\ldots\ldots\ldots\ldots\ldots(1.1)$$

$$\therefore \text{ Annual rate of collapse} = \frac{293}{10} = 29.3$$

The annual rate of the total collapse over the period of 2005 to 2014 is found to be 29.3 collapses. As observed from the bar chart in figure 1.2, the problem of voltage collapse is enormous as it occurs at an annual rate of 29.3 collapses within the 10-year period i.e. approximately, twenty nine (29) collapses per year making the entire power system network insecure and unreliable.

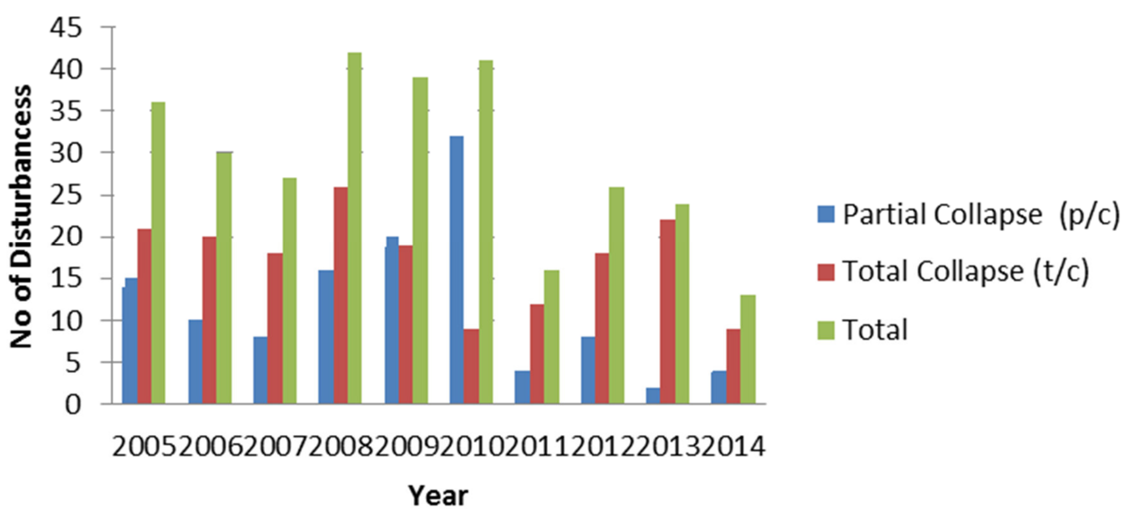

Figure 1.2: Bar chart showing the NNG system disturbances from 2005 to 2014 (Samuel *et al.,* 2014 (a))

Table 1.2 shows a classification of system collapses on the NNG system. The disturbances that are responsible for the higher number of system collapses are fault induced and these are about 88%. It can be inferred that the NNG is weak and vulnerable to voltage collapse or instability (Samuel *et al.,* 2014 (a)).

Table 1.2: Classification of system collapses 2008-2010 on the NNG

Nature of Disturbances	2008	2009	2010
Faults	36	33	118
Gas (low pressure or lack)	2	5	0
Overload	1	2	3
Frequency	2	0	2
Unknown reason	1	0	0

Source: Samuel *et al.,* 2014 (a)

Consequently, this study is motivated by the severity of voltage instability when it occurs and the need to have a fast and accurate indicator for its prediction. Hence, the need to develop and derive a reliable voltage stability index for PSN's voltage stability monitoring and prediction arises. More importantly, voltage magnitude alone is not sufficient to determine the optimal deployment of compensation devices for control purposes hence the use of line stability index, which is a good indicator of voltage instability (Subramanian and Ravi, 2011). In view of the inadequacies discovered with some of the existing indices in literature, the present study will attempt to develop a novel voltage stability index.

The monitoring of voltage stability for a power grid is an onerous function for the grid operator, hence the use of indices to determine and /or predict the system stability state. These indices are scalar quantities that are observed as system parameters change. Hence, operators use these indices to know when the system is close to voltage collapse. the indices are used to take corrective measures to avert the voltage collapse thereby sustaining the continuous supply to consumers and to know the vulnerable line with respect to a bus for location of possible compensation devices for mitigating voltage instability (Chayapathi, *et al.,* 2013).

1.5 Scope of Research Work

The scope of this research work is limited to the study of voltage stability and prediction of voltage collapse on PSNs with line stability indices.

This research work focuses on the prediction of voltage collapse on PSN using a developed voltage stability line index. The study helps to identify the weak bus, critical lines with respect to a bus in order to determine the optimum placement of compensation devices and voltage collapse relay on the PSN and to investigate the effect of increasing reactive power loading on the power system network. The developed index is tested on simulated model of IEEE 14-bus system for validation of the index and then investigated on the simulated model of the present 28-bus, 330-kV NNG. The simulations were carried out in the MATLAB, R2012a (7.14.0739) 32-bit (win32) environment.

1.6 Thesis Organization

The rest of the thesis is organized as follows:

Chapter two presents an overview of power system stability and a review of voltage stability indices. Chapter three focuses on derivation of the novel voltage stability index being proposed for voltage collapse prediction. Chapter four validates the newly proposed line stability index and presents simulation results and discussions while Chapter five presents the conclusions drawn from the study and proffers suggestions for further work.

CHAPTER TWO

LITERATURE REVIEW

2.1 Introduction

This chapter provides an overview of the relevant technical literature related to the present study. It begins by defining power system stability and its classification. The major voltage collapse incidences across the world are reviewed. Differentiation is made between rotor angle and voltage stabilities. The five states of a PSN are reviewed together with the existing line stability indices for predicting voltage instability.

2.2 Power System Stability

A power system is a complex dynamic system made up of linear and nonlinear subsystems and constantly subjected to internal and external disturbances. Power system stability can be defined as the ability of the power system to remain in state of equilibrium under normal operating conditions and to regain an acceptable state of equilibrium after being subjected to a disturbance (Kundur, 1994).

According to the IEEE/CIGRE, joint task force (in Kundur *et al.,* 2004), "Power system stability is the ability of an electric power system, for a given initial operating condition, to regain a state of operating equilibrium after being subjected to a physical disturbance, with most system variables bounded so that practically the entire system remains intact." Figure 2.1 shows the classification of power system stability according to the IEEE/CIGRE joint task force.

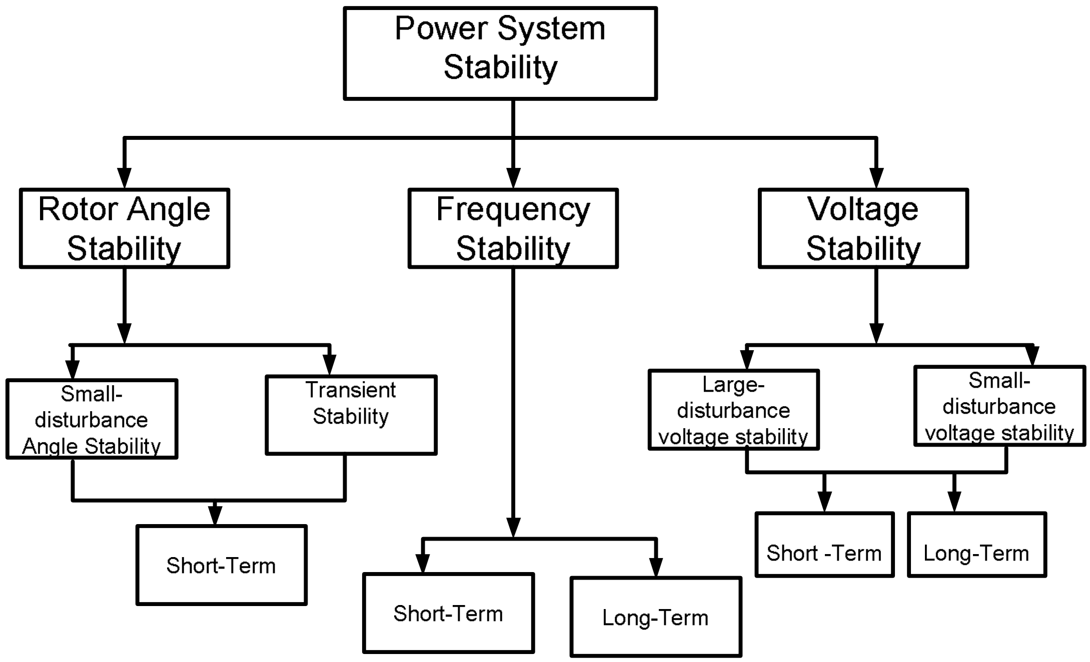

Figure 2.1: Classification of power system stability (Kundur *et al.,* 2004)

2.2.1 The Basic Forms of Power System Stability

The three basic forms of power system stability are rotor angle, frequency and voltage stabilities. These terms are discussed in the following sub-sections:

2.2.1.1 Rotor Angle Stability

Rotor Angle stability of a power system is the ability of interconnected synchronous machines of the power system network to remain in step with one another i.e. in synchronism (Kundur, 1994). The rotor angle stability problem involves the study of electro-mechanical oscillations. The fundamental factor of rotor angle stability is the manner in which power output of a synchronous machine varies with rotor oscillation. This could either be steady-state stability or transient state stability.

2.2.1.2 Frequency Stability

Frequency stability refers to the ability of a power system to maintain steady frequency following a severe system upset resulting in a significant imbalance between generation and load. It depends on the ability of the network to maintain or restore equilibrium between system generation and load, with minimum unintentional loss of load. Generally, frequency stability problems are associated with inadequacies in equipment responses, poor coordination of control and protection equipment, or insufficient generation reserve (Kundur, 1994 and Kundur, *et al.,* 2004). Frequency stability could be short-term (which ranges from a fraction of a second) or a long-term phenomenon as shown in figure 2.1.

2.2.1.3 Voltage Stability

Voltage stability is concerned with the ability of the power system to maintain acceptable voltage levels at all buses in the system under normal operating conditions and after being subjected to disturbances (Kundur, 1994). This involves finding the voltage level at each bus at different loading conditions to know the stability limits and margin. Due to the heavy economic and social effect of voltage instability on the utility company and customers, a lot of research work is being done across the globe. Based on the size of the disturbance, voltage stability can be further classified into the following two subcategories:

a. Large-disturbance voltage stability refers to the system's ability to maintain steady voltages following large disturbances such as system faults, loss of generation, or circuit contingencies.
b. Small-disturbance voltage stability refers to the system's ability to maintain steady voltages when subjected to small perturbations such as incremental changes in system load.

The time frame of interest for voltage stability problems may vary from a few seconds to tens of minutes. Voltage stability may either be a short-term or a long-term phenomenon as discussed below:

i. Short-term voltage stability involves dynamics of fast-acting load components such as induction motors, electronically controlled loads, and HVDC converters. The study period of interest is in the order of several seconds.

ii. Long-term voltage stability involves slower-acting equipment such as tapchanging transformers, thermostatically controlled loads, and generator current limiters. The study period of interest may extend to several or many minutes. Note that long-term simulations are required for analysis of system dynamic performance (Kundur *et al.,* 2004; Ajjarapu and Meliopoulos, 2008).

2.3 Difference between Angle Stability and Voltage Stability

Traditionally, the power system stability issue has been the rotor angle stability, i.e. maintaining synchronous operation in the PSN. Instability in PSN may also occur without loss of synchronism in the PSN. The rotor angle stability problem involves the study of electro-mechanical oscillations (Bhaladhare *et al.,*2013). A power system is voltage stable if its bus voltages after a disturbance are close to voltages at normal operating conditions and it becomes unstable when voltages uncontrollably decrease due to outage of equipment or increment of load. Voltage stability and rotor angle stability are interrelated. Meanwhile, the rotor angle stability as well as voltage stability are affected by reactive power control. Voltage stability is basically load dependent and rotor angle stability is basically generation dependent. It can be said that angle stability related issues are encountered when the balance between real power generation and the load is not zero. On the other hand, voltage stability related problem is encountered in the system when the balance between the reactive power generation and load is not zero.

2.4 Voltage Collapse Incidences

Voltage collapse may be the resultant effect of voltage instability in a PSN. Voltage instability is the process by which voltage falls to a very low value as a result of series of events. The world has witnessed several voltage collapse incidences in the last decades – prominent incidents that attracted much attention happened in Belgium (August, 1982), Sweden (December, 1983), Tokyo (July, 1987), Tennessee (August, 1987) and Hydro Quebec (March, 1989), Andersson *et al.,* (2005), Pourbeik *et al.,* 2006). Many major blackouts caused by voltage instability have illustrated the importance of this phenomenon (Kundur, *et al.,* 2004) and (Taylor, 1994). In view of the present deregulation of the electrical power industry worldwide, power systems have evolved through continuing growth in interconnections resulting in more complexity, use of new control technologies, and in the increased operation in highly stressed conditions. This has given rise to different forms of system instability.

The bar chart of Figure 2.2 shows the total number of collapses throughout the world and it also shows its growth and the increasing trend.

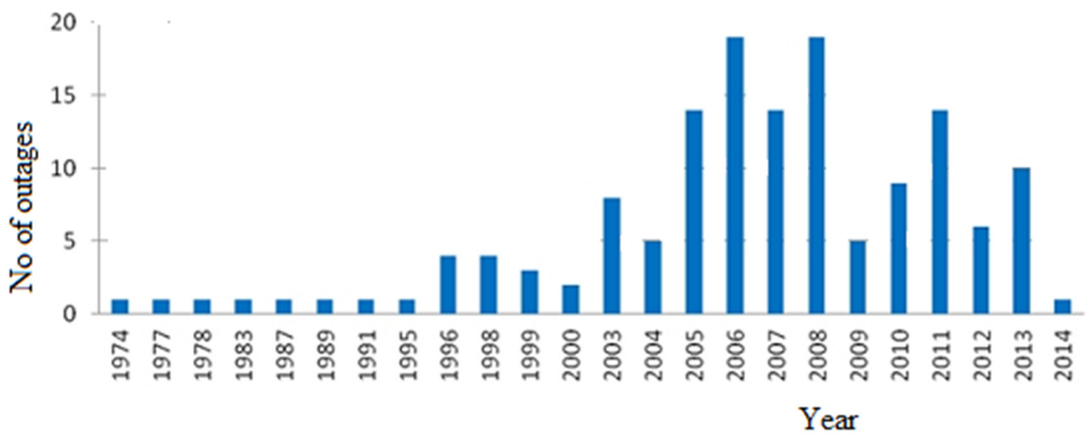

Figure 2.2: Worldwide voltage collapse 1974 - 2014 (Goh *et al.,* 2014)

The blackouts that occur in the United States (U.S.) and in Canada on the 14th of August, 2003 have proven to be the most severe and significant (Andersson *et al.,* 2005) It was reported that during the blackout, about 50 million people were affected in eight states of the United States and two Canadian provinces. Approximately, 63 GW of load was lost, which is about 11 % of the total load. Also, in Southern Sweden, a major system collapse took place on 23rd September 2003, and impacted up to 4 million customers (Pourbeik, 2006). Some other major blackouts began when a tree flashover caused the tripping of a major tie-line between Italy and Switzerland (Goh, *et al.,* 2014). The NNG also witnessed several collapses according to Transmission Company of Nigeria's (TCN) records. Table 2.1 shows a sample of the records for the year 2009 showing the summary of major system disturbances in 2009 (Power Holding Company of Nigeria, 2010; TCN, 2015).

TABLE 2.1: Summary of Major System Disturbances in 2009

S/No	Date	Duration (Hrs)	Type of Disturbances	CAUSES / REMARK
1	16/01/09	0.82	Total Collapse	The sudden low gas pressure at Egbin/aes power station resulting in rejection of 631.7MW Egbin/aes generation
2	06/02/09	0.55	Partial Collapse	The tripping of Afam iv/Afam v 330kV tie and line circuit breakers (18ac q01 and 18ac q02) at Afam vi end p.s on differential protection resulting in rejection of 300MW generation. Only Geregu p.s. Feeding Lokoja, Okene,Irrua, Ukpilla, Agbor and Ajaokuta complex survived the collapse.
3	13/02/09	0.47	Partial Collapse	The tripping of Jebba/Osogbo 330kV circuit j2h due to heavy surge. Egbin and Geregu with total load of 357MW survived the collapse.
4	23/02/09	0.23	Partial Collapse	The tripping of Osogbo/Benin 330kV line (cct. H7b). This split the grid into two. The thermal, Geregu and Omoku with total load of 1635.4MW survived the collapse.
5	24/02/09	1.67	Partial Collapse	(I) the tripping of benin t/s 2 x 150MVA 330/132/33kV transformer (6t1 & 6t2) secondary breakers on e/f and Benin/Irrua 132kV line on d/p, e/f zone 1, which resulted to frequency rise from 50.32hz to 51.68hz. (ii) The tripping of Okpai p/s st1 on high frequency.
6	25/02/09	2.17	Partial Collapse	(I) the tripping of Omotosho/ Ikeja West 330kV line (cct. M5W) at Omotosho t/s on line fault. Nb: cct. H7b, b6n & r2a were out on line fault.

S/No	Date	Duration (Hrs)	Type of Disturbances	CAUSES / REMARK
7	07/03/09	0.28	Partial Collapse	The tripping of Egbin p/s (st1-st5) units and aes p/s gt202-205,208-211) due to lack of gas supply as a result of fire outbreak at ngc (load lost 710.5 MW)
8	13/03/09	0.37	Partial Collapse	(I) the tripping of Benin/Onitsha 330kV line (cct.b1t) cb1 (ii) the tripping of Okpai p/s st1 and Afam vi p/s rejecting about 698MW
9	16/03/09	0.32	Partial Collapse	Delta g.s. Units (gt6, 8, 9, 10, 11, 12, 14, 18 & 20) tripped as result of sharp drop on gas pressure (2.04mpa to 0.10mpa), rejecting a total load of 305MW.
10	17/03/09	0.57	Partial Collapse	Over loading of the grid. Geregu and Omoku p.s. Of 162MW survived the collapse.
11	07/04/09	0.50	Partial Collapse	The tripping of Benin/Onitsha 330kV line (cct. B1t) at e/f, red phase, zone 3 trip. Onitsha end only on ohmega.
12	11/4/09	2.07	Partial Collapse	The tripping of Benin/Onitsha 330kv line (cct. B1t) on earth fault rejecting 166MW power import into Benin t.s.
13	16/4/09	0.32	Partial Collapse	Over loading of the grid.
14	02/05/09	1.23	Partial Collapse	**(A)** the multiple tripping of the following: (1) sapele/benin 330kV lines (ccts. S3b & s4b),(2) Osogbo/Benin 330kV line(cct h7b) (3) Benin/Egbin 330kV line(cctb6n), (4)Benin/Omotosho 330kV line (cct b5m) (5)Shiroro 330kV transformer tr2 and Katampe 330kV transformer tr1 & tr2 on differential relay & **(b)** the explosion of vt on blue phase of Shiroro/Mando 330kV line(cct r1m) at

S/No	Date	Duration (Hrs)	Type of Disturbances	CAUSES / REMARK
				Mando.
15	03/05/09	0.28	Partial Collapse	Simultaneous tripping of the following lines due to explosion of red phase c.t. At Osogbo t.s: (1) Osogbo/Ikeja West 330kV line(cct h1w), (2) Jebba/Osogbo 330kV line(cct j1h), (3) Osogbo/Ayede 330kV line(cct h2a), (4) Osogbo/Benin 330kv line (cct h7b)
16	13/05/09	0.52	Partial Collapse	1. Shiroro/Katampe 330kV lines (ccts. R4b & r5b) were opened on control due to the tripping of 2 x 150MVA 330/132/33kV transformer (t1 & t2) at Katampe t.s. 2. Simultaneous tripping of the following: (a) Shiroro/Katampe 330kV lines (ccts. R4b & r5b) due to explosion of red phase lighting arrester at Shiroro t.s. As a result of high voltage of 400kV. (b) Jebba/Ganmo 330kV line (cct. J3g) and Jebba/Shiroro 330kV lines i & ii (ccts. J3r & j7r) at Jebba t.s. But (cct. J3r) tripped also at Shiroro t.s. (c) 2 x 150mva 330/132/33kV transformer (t1 & t2) at Shiroro t.s. On differential potential.
17	19/05/09	1.13	Total Collapse	Emergency opening of Benin/Onitsha 330kV line (cct. B1t) as a result of burning of blue phase line isolator at Benin t.s.
18	29/05/09	0.38	Total Collapse	At 1420hrs, Okpai st1 tripped due to problem on its two(2) boilers, rejecting 144mw. While gt11 & 12 deloaded to house load rejecting 302mw. Total generation of 446MW

S/No	Date	Duration (Hrs)	Type of Disturbances	CAUSES / REMARK
				was lost.
19	20/06/09	0.62	Total Collapse	Trippings of Afam vi gt12 on overspeed with load loss of 146MW and circuit breaker of gt11 with load loss of 147MW were reported. Total load loss was 293mw.
20	21/06/09	0.42	Total Collapse	Onitsha/Alaoji 330kV line (cct t4a) tripped, Afam vi generation of 291MW was lost. Despite effort to maintain stable system frequency through load shedding there was instability in the system. Okpai then reduced their generation from 228MW to house load.
21	22/06/09	0.37	Total Collapse	Over loading of the grid
22	23/06/09	0.73	Total Collapse	Onitsha/Alaoji 330kV line (cct t4a) tripped at Onitsha end, cut-off Afam vi generation (gt11 & 12) of 197MW towards Onitsha t.s.
23	24/06/09	0.45	Total Collapse	Delta/Benin 330kV line (cct g3b) tripped at both ends, cut-off delta generation of 281MW
24	27/06/09	0.75	Total Collapse	(1) attempts to restore Shiroro/Mando 330kV line 1 (cct. R1m) to improve system security and voltage, developed pole discordance fault at 0846hrs. (2) The bus zone protection scheme thereby cleared all the 330kV ccts at Mando t/s, namely r2m, m6n & m2s. (3) The trippings led to frequency fluctuation and voltage escalation. (4) Okpai deloaded from 234MW to 93MW due to frequency fluctuation at 0847hrs to the time of system collapse.

S/No	Date	Duration (Hrs)	Type of Disturbances	CAUSES / REMARK
25	03/07/09	1.73	Total Collapse	(A) Tripping of the following lines: (1). Jebba/Osogbo 330kV line (cct j1h) at Jebba end on fault (2). Jebba/Ganmo 330kV line (cct j3g) at Jebba end on fault (3). Benin/Onitsha 330kV line (cct b1t) at both end . (b) Tripping of Afam 11 p.s., gt5 64MVA 132/11kV power transformer on over current (o/c) due to fire out break at 11kV control room.
26	07/07/09	0.85	Total Collapse	Loss of generation due to low gas pressure from delta p.s suspected. Delta gt20 tripped between (1201 - 1209), follow by report of low gas pressure from the station.
27	22/07/09	0.45	Total Collapse	Benin/Onitsha 330kV line (cct bit) tripped at both ends, cut-off 363MW export from Onitsha end
28	29/07/09	0.27	Total Collapse	The tripping of Shiroro/Kaduna 330kV line 2 (cct. R2m) at Mando t.s. Only on Optimho relay, distance protection zone 2, abc, delay and baj 86a, 86b, 86c.
29	14/08/09	0.37	Partial Collapse	Osogbo/Benin 330kV line(cct h7b) tripped at both ends
30	17/08/09	0.35	Total Collapse	The simultaneous tripping of Onitsha/Alaoji 330kV line (cct. T4a) at both ends and Jebba/Shiroro 330kV lines 1 & 2 (ccts j3r and j7r) at Jebba t.s only.
31	19/08/09	2.58	Total Collapse	Afam vi p.s (low gas pressure) rejecting 442MW generation
32	20/08/09	0.37	Total Collapse	The tripping of Jebba/Shiroro 330kV lines (cct j3r & j7r), and Jebba power station 330kV line 1(cct. B8j) simultaneously, resulting in the separation of Jebba g.s units 2g1, 3 &

S/No	Date	Duration (Hrs)	Type of Disturbances	CAUSES / REMARK
				4 on system surge, rejecting a total load of 299MW.
33	26/08/09	0.88	Total Collapse	The tripping of Afam/Alaoji 330kV line 1 (cct f1a) at Alaoji end separated Afam g.s from the grid with a total generation of 469MW.
34	08/09/09	0.50	Total Collapse	The tripping of Afam/Alaoji 330kV line(cct.f1a) at Alaoji t.s due to jumper cut on Afam/Portharcourt 132kV line resulting in loss of Afam vi g.s units gt 12 & 13 on over speed with load loss of 300MW
35	11/10/09	6.37	Partial Collapse	As indicated on the ncc scada mmi, delta p.s and Egbin p.s suspected tripped with total generation loss of 415MW
36	16/10/09	0.28	Partial Collapse	At 15:00hrs Benin/Egbin 330kV line, (cct. B6n) tripped at both ends at 14:57hrs Omotosho tie cb tripped simultaneously and separated 330kV cct b5m and m5w, note: at 14:40hrs cct. H7b tripped earlier before the collapse.
37	05/11/09	1.18	Total Collapse	Tripping of the following lines at 14:39hrs: (1) Onitsha/Alaoji 330kV line, (cct. T4a) at both end (2) Jebba/Shiroro 330kv lines 1 & 2 (cct. J3r & j7r) (severing Shiroro generation of 282MW)
38	08/12/09	0.82	Total Collapse	Emergency opening of Jebba g.s./Jebba t.s. 330kV lines 1 & 2 (ccts b8j & b9j) at Jebba t.s. - due to "fire outbreak" - at the instance of Jebba g.s., thereby cutting off Jebba g.s. Generation of 347MW. The incident was later reported to be a flashover on unit 2g4 discharge resistor. It was not

S/No	Date	Duration (Hrs)	Type of Disturbances	CAUSES / REMARK
				a fire outbreak.
39	24/12/09	1.22	Partial Collapse	The tripping of Benin/Omotosho 330kV line (cct. B6n) at Benin t.s. Ends, thereby separating the grid into 2 islands.

Source: Power Holding Company of Nigeria 2010; TCN, 2015

Voltage collapses have attracted special attentions to maintain the stability of the transmission networks in order to avoid recurrence of major blackouts as experienced by the above mentioned countries. Hence, research work in this area is aimed at predicting voltage collapse with a view to reducing its occurrence on PSNs.

Figure 1.2 and Figure 2.3 were combined for the comparative assessment of the global outages and the NNG. Table 2.3 shows the comparative analysis of the globe outage and the outages on the NNG.

Table 2.2: Comparative Analysis of Global and the NNG Outages

Year	2005	2006	2007	2008	2009	2010	2011	2012	2013	2014
NNG Total No of Collapse	36	30	26	42	39	41	16	26	24	13
Global total No of collapse	14	18	14	18	14	9	14	6	10	2

*NNG- Nigerian National Grid

The bar chart of Figure 2.3 shows comparative voltage collapses between 2005 – 2014 for Global and the NNG voltage collapses. This reveals that the NNG experiences more voltage collapses than what obtains globally. This brings to bear the enormity of the problem on the Nigeria National grid system and therefore, the need arises to carry out research to ensure reduction in the voltage collapse.

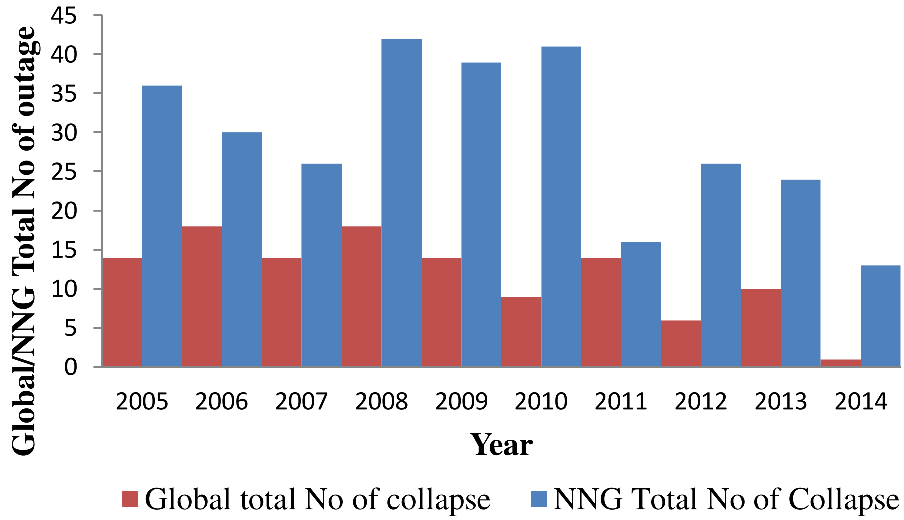

Figure 2.3: Comparative voltage collapse 2005 - 2014: Global and the NNG

2.5 Voltage Stability Analysis

In general, the methods used in carrying out voltage stability analysis are categorized into two, namely, dynamic and static stability analyses.

2.5.1 Dynamic Methods

These employ nonlinear differential and algebraic equations (DAE) in the power system model. For large disturbances, which include generator dynamics, tap changing transformers, etc, the DAEs, are solved through transient stability simulations and the system response over a certain period of time is observed. Dynamic analysis is very important for system control.

2.5.2 Static or Steady-State Stability Methods

In static analysis, the system is assumed to be in steady state and hence only the algebraic equations are considered. This type of analysis is suitable for small-disturbances in the system and it uses the conventional power-flow model. The static analysis is useful for indicating the possibility of voltage collapse and proximity of the system to collapse (Kundur *et al.,* 2004).

Static analysis is required when there are fluctuations in load. This includes the normal slow random load fluctuation. In this case, the equilibrium point of the system moves slowly and makes it possible to approximate voltage profile changes by a discrete sequence of steady states rather than using a dynamic model (Nizam *et al.,* 2007).

In the static analysis of voltage stability, the snapshots of the entire system at different instants are considered and at each instant, the system is assumed to be in steady state and that the rates of changes of the dynamic variables are zero. Hence, instead of considering all the differential algebraic equations, only the algebraic power balance equations are considered assuming that the system is in steady state. At each instant whether the system is voltage stable or not, how far the system is from instability can be assessed (Morison, *et al.,* 1993; Vadivelu and Marutheswar, 2014). Although stability studies in general require a dynamic model of the power system, static analysis techniques have been found to be widely used for voltage stability analysis (Quintela and Castro, 2002). In this research work, the static analysis model has been used.

2.6 The Operating States of an Electric Power System

In the wake of the 1965 Northeast blackout in the US, the electric power system community engaged in research and development aimed at modernizing the monitoring, protection and control of the electric power generation, transmission and distribution subsystems. This endeavor resulted in much methodological and technological advancement, which include the following:

(i) The provision of the control centers with mainframes and, later on, distributed computers.

(ii) The initiation of a theoretical framework along with an ensemble of computer-aided functions to partially automatize the operation of the transmission system.

(iii) The development of fast algorithms based on sparse matrix techniques for modeling the steady-state and the dynamic operating conditions of the system.

The theoretical framework was set up by Dy Liacco (Liacco, 1967) and then Fink and Carlsen, (1978) worked on the definitions of five operating states of a power system as depicted in Fig.2.4. These are the normal, alert, emergency, in extremis, and restorative states.

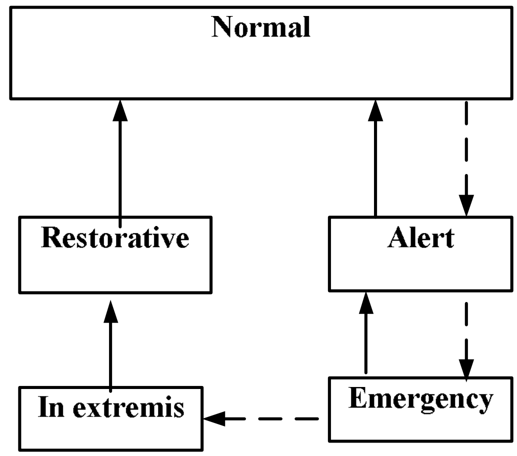

Figure 2.4: The five states of power system and their transitions (Lamine, 2011)

System operation in steady state is governed by equations which express

- Equality Constraints (E), Real and Reactive power balance at each node
- Inequality Constraints (I), Limitations of physical quantities, such as currents and voltages must not exceed maximum limits.

The five states of power system are thus defined as follows:

(i) **Normal state**: This state could be referred to as secured state. It satisfies all the equality (E) and inequality(I) constraints and sufficient level of stability margins in transmission and generation so that the system can withstand a single contingency, be it a loss of a transmission line, a transformer, or a generator. In this case, the system state is said to be secure. The generation is sufficient to supply the existing load demand and no equipment is overloaded.

(ii) **Alert state:** It is a state symbolized by the satisfaction of all the equality and inequality constraints and by an insufficient level of stability margins, which is an indication that the system is dangerously vulnerable to failures. This implies that there is a danger of violating some of the inequality constraints when subjected to disturbances (stresses) such as transmission line or transformer overloading. Preventive step is required to bring the system to normal state by ensuring that redundancy in the transmission line is increased.

(iii) **Emergency state:** It is a state where all the equality constraints are satisfied and at least one inequality constraint is violated. The state is entered into due to a severe disturbance, arising from the system experiencing overloads. Obviously, the system calls for the immediate implementation of corrective actions to remove the overloads, prevent damage of equipment, and mitigate the risk of cascading failures that may lead to total collapse. These actions consist of load shedding, transmission line tripping, transformer outages, or generating unit disconnections.

(iv) **In extremis state:** This is characterized by the violation of both equality and inequality constraints that stem from the chain of actions taken at a previous emergency state while the transmission network remains interconnected. Emergency control action should be directed at avoiding total collapse.

(v) **Restorative state:** This is a transitional state in which inequality constraints are met from emergency control actions taken but the equality constraints are yet to be satisfied. From this state, the system can transmit to either the alert or the normal state depending on the circumstances. Here, restorative actions need to be implemented to bring the system to a normal or alert state.

Due to the fact that power system is dynamic in nature, changing its characteristics may lead to its operating point to be dangerously driven close to the stability limits of the basin of attraction of its current stable equilibrium point. In other words, the safety margins of a power system may quickly erode with time as the internal and external conditions evolve. Consequently, a continuous assessment of the stability margins of the system has to be executed to check whether it is still in a normal state (Padiyar, 1996; Lamine, 2011)**.**

The NNG is reported to operate perpetually in the alert state as against the Grid Code stipulation that the grid has to be in the normal state at least 90% of the time

(Ndiagwalukwe, 2012) and had remain at this level to date as most transmission line project are still under construction. Hence, it becomes important to continuously monitor the PSN to ensure that voltage stability is not violated.

2.7 Voltage Stability Indices

There are varieties of tools for assessing whether a system is voltage stable or not and how close the system is to instability. These tools are called voltage stability indices. These indices help the system planner and operators to know the condition of voltage stability in a power system. They indicate how close the system is to voltage collapse or instability. The indices should be simple, easy to implement and computationally inexpensive. The indices expose the critical bus of a power system and the stability condition of each line connected between two buses in an interconnected network (Kumarswamy and Ramanareddy, 2011; Mathew *et al.,* 2015). In general, the analysis of the voltage stability problem of a given PSN should:

- determine the system's proximity to collapse.
- establish when the voltage instability could occur.
- identify the weak buses in the PSN
- identify the areas involved.

2.7.1 The P-V Curve and Q-V Curve

The P-V curves are used to determine the loading margin of a power system. Figure 2.5 shows a P-V diagram of a power system at a particular operating point, with the two solution points. The upper V_U is the normal operating point, but a solution at V_L is also possible. It can be seen that the distance (ΔV) between the two solutions tends to zero as the margin of power P_m between the operating point and the point of maximum power approches zero. The Q-V curve can be used as an index for voltage instability, the point where dQ/dV is zero is the point of voltage stability limit. Figure 2.6 shows the Q-V curves for a bus in a particular power system for three different loads: P_1, P_2 and P_3. (Chawla and Singh, 2013). The vertical axis shows the amount of additional reactive power that must be injected into the bus to operate at a given voltage. The operating point is the intersection of the power curve with the horizontal axis, where no reactive power is required to be injected or absorbed (Bhaladhare *et al.,* 2013; Balamourougan *et al.*2004; Sanaye-Pasand and Rezaei-Zara, 2003).

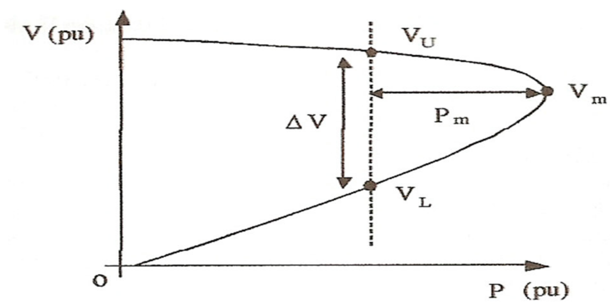

Figure 2.5: P-V curve (Sanaye-Pasand and Rezaei-Zara, 2003)

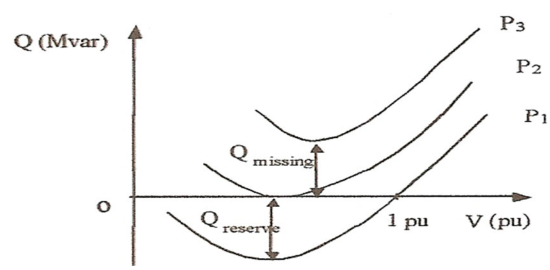

Figure 2.6: Q-V curves for three loads (Sanaye-Pasand and Rezaei-Zara, 2003)

2.7.2 Modal Analysis

The voltage stability of a power system may be deduced from a consideration of the eigenvalues and eigenvectors of the system's reduced power-flow Jacobian matrix (Gao *et al.*, 1992; Bhawana and Prabodh, 2015). Such eigenvalues are associated with system voltage modes as well as the reactive power variation. In the steady-state, a power system is said to be voltage stable if all the eigenvalues of the reduced power-flow Jacobian matrix are positive and if any of the eigenvalues is negative, then it is unstable (Bhawana and Prabodh 2015; Enemuoh *et al*, 2013). For the reduced power flow Jacobian matrix, a zero (0) eigenvalue means that the system is on the borderline of voltage collapse. It implies that there is a likelihood of voltage instability situation (Gunadin *et al*, 2012).

The PV and QV, the modal analysis and energy-based methods as proposed by Hasani, & Parniani (2005) and Nizam *et al*, (2007) are computationally tedious, rigorous and time consuming whereas time is of essence when dealing with voltage collapse prediction. So, the use of less tedious, computational fast and easy-to-use voltage stability indices for online and offline prediction of voltage collapse are preferred.

2.7.3 L- Index (L)

Kessel and Glavitsch, (1986) developed L-index based on the power flow solutions. It measures the proximity to voltage instability and it is appropriate for constant power load type. Its value ranges from zero (0) – no load to unity (1) collapse point (Suganyadevia and Babulalb, 2009). L-index is given as

$$L = \max_{j \in \alpha L}\{Lj\} = \max_{j \in \alpha L}\left\{\left|1 - \frac{\sum_{i \in \alpha_G} F_{ji} * V_i}{V_j}\right|\right\} \tag{2.1}$$

$$F_{ji} = |F_{ji}| \angle \theta_{ji}$$

where L is the set of consumer nodes and G is the set of generator nodes, Lj is a local indicator that determines the busbars from where collapse may originate (Kessel and Glavitsch, 1986). The [F] is computed using $[F] = [Y_{LL}]^{-1}[Y_{LG}]$, where $[Y_{LL}]$and $[Y_{LG}]$ are sub-matrices of the Y-bus matrix. the voltages V_i and V_j are voltages at buses i and j respectively (Tiwari *et al.,* 2012 and Vadivelu and Marutheswar, 2014).

2.7.4 Line Stability Index (Lmn)

Line stability index (Lmn) is derived based on power transmission line concept in a single line. Moghavvemi and Omar (1998) derived this line stability index to evaluate the stability of the line between two buses in an inter-connected system reduced to a single-line network as shown in Figure 2.7

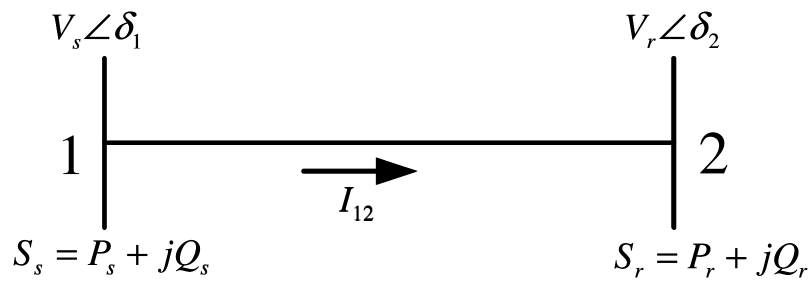

Figure 2.7: Typical one-line diagram of transmission line.

Where, Vs, Ps and Qs are the sending-end voltage, real power and reactive power, are respectively. Vr, Pr and Qr are the receiving-end voltage, real power and reactive power respectively. δ_1 is the sending-end voltage phase angle and δ_2 is the receiving-end voltage phase angle, I_{12} is the line current and θ is the transmission line angle.

The power flow through a transmission line using pie (п) model representation for a two-bus system is used and the discriminant of the voltage quadratic equation is set to be greater than or equal to 0 (zero). If the discriminant is less than 0 (zero), the roots will be imaginary suggesting that there is instability in the system. The expression for the index is given as

$$Lmn = \frac{4XQ_r}{|V_s|^2 \sin^2(\theta - \delta)} \leq 1 \qquad (2.2)$$

The line index is also directly related to the reactive power and indirectly related to the active power through the voltage phase angle δ. A line in the system is said to be close to instability when the Lmn is close to one (1). On the other hand, if the Lmn value is less than 1, then the system is said to be stable (Moghavvemi and Omar, 1998).

2.7.5 Fast Voltage Stability Index (FVSI)

This index, proposed by Musirin and Rahaman (2002), is also based on the concept of power flow through a single line (Mathew, *et al.,* 2015) as shown in Figure 2.6. It was developed based on the measurements of voltage and reactive power. In its derivation, the sending bus is taken as the reference bus with the voltage phase angle set to zero. FVSI is a line index derived from the general equation for the current in a line between two buses, labeled ‘s’ and ‘r’. Its mathematical expression is given as

$$FVSI = \frac{4Z^2 Q_r}{V_s^2 X} \leq 1 \tag{2.3}$$

where Z is the line impedance, X is the line reactance, Q_r is the reactive power flow to the receiving end and Vs is the sending-end voltage. The line whose stability index value is closest to unity (1) will be the most critical line of the bus and may lead to the whole system instability (Verayiahah and Marutheswar, 2013). The evaluated FVSI also helps to determine the weakest bus in the system. The most critical bus in the system is the bus with smallest permissible load (Moghavvemi and Omar.1998).

2.7.6 Line Stability Factor (LQP)

The LQP index derived by Mohamed*, et al*, (1989) is obtained using the same concept as in Moghavvemi and Omar, (1998) and Musirin and Rahman, (2002) in which the discriminant of the power quadratic equation is set to be greater than or equal to zero. Figure 2.6 illustrates a single line of a power transmission concept used in the formation of the index. The line stability factor for this model is reproduced as

$$LQP = 4\left(\frac{X}{V_s^2}\right)\left(\frac{X}{V_s^2} p_s + Q_r\right) \tag{2.4}$$

where X is the line reactance, Qr is the reactive power flow to the receiving bus, V_s is the voltage at the sending bus and P_s is the active power flow from the sending bus. For stable system, the value of LQP index should be maintained at less than 1, otherwise, collapse is imminent (Mohamed *et al*, 1989).

2.7.7 Line Voltage Stability Index (LVSI)

This index is a line voltage stability index that brings to bear the relationship between line real power and the bus voltage (Suganyadevi and Babalal, 2009). The index fails if the resistance of the transmission line is very close to zero. The index is formulated as

$$LVSI = \frac{4RP_r}{V_s \cos\theta - \delta} \leq 1 \tag{2.5}$$

where

$\theta = \tan^{-1}\dfrac{X}{R}$ is the transmission line angle and R is line resistance

LVSI is more sensitive to δ since cos(θ-δ) is faster than sin(θ-δ) around 90^0 and a healthy line could be identified as a critical line (Haruna, 2015).

2.7.8 Voltage Collapse Point Indicator (VCPI)

The VCPI uses maximum power transfer concept to investigate the stability of each line of the PSN. The expressions for the indices are stated as follows:

$$VCPI\,(power) = \frac{P_R}{P_{R(\max)}} \tag{2.6}$$

$$VCPI\,(Losses) = \frac{P_{Losses}}{P_{Losses(\max)}} \tag{2.7}$$

where P_R is the power at the receiving end and P_{losses} is the power loss.
As the transmission line experiences increase in power flow transfer, the value of each of the indices in equations (2.6) and (2.7) increases gradually and if it reaches 1, the voltage collapse occurs and if the index of any line in the PSN reaches that value, it is possible to predict the voltage collapse. The VCPI indices vary from zero (0) no-load condition to one (1), which is voltage collapse (Goh, *et al.,* 2015).

2.9 Summary

Power system stability i.e. the rotor angle, frequency and voltage stability were reviewed. Rotor angle and voltage stability interrelationship were briefly discussed. Existing voltage stability indices in the literature as well as the power system operational security states were outlined.

CHAPTER THREE

MATERIALS AND METHODS

3.1 Introduction

In this chapter, a new line stability index, NLSI-1 is proposed for PSN voltage collapse prediction. This chapter presents the mathematical formulation for the proposed index. The methods and materials for the study are also presented.

3.2 The New Voltage Collapse Prediction Index

Voltage stability, to a very large extent, has to do with system load and transmission line parameters, indices that reveal how close each transmission line is to voltage instability have increasingly become essential tools for voltage stability assessment and monitoring by power system operators. These indices may be used for online or offline monitoring of the PSN in order to predict proximity to voltage instability or collapse.

3.2.1 New Line Stability Index-1 (NLSI-1)

To derive the New Line Stability Index-1 (NLSI-1) we first consider the Line Stability Index (Lmn) proposed by Moghavvemi and Umar, (1998) and the Fast Voltage Stability Index (FVSI) proposed by Musrin and Rahman, (2002). We then showed that the FVSI is an approximation of the Lmn and proceed to derive the NLSI-1 for improved accuracy and speed.

Consider the one-line diagram of a two-bus power system model shown in figure 3.1. All parameters and variables are in per unit.

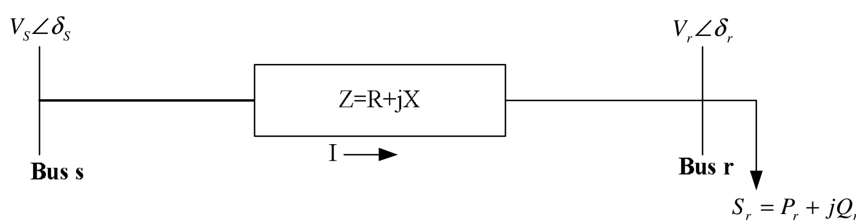

Figure 3.1: One-line diagram of a two-bus power system model

In Figure 3.1, bus ‘s’ is the sending-end bus and is chosen to be the reference bus while bus ‘r’ is the receiving-end bus. The variables and parameters are defined as follows:

S_r is the apparent power at the receiving bus ‘r’.

P_r is the real power at the receiving bus ‘r’

V_s , V_r are respectively the sending-end voltage and the receiving-end voltage.

Q_r is the reactive power at the receiving bus ‘r’.

δ_s , δ_r are respectively the voltage angles of the sending-end and the receiving-end buses.

δ is the difference between δ_s and δ_r

$\theta = tan^{-1}\frac{X}{R}$ is the transmission line angle

$\overline{z} = R + jX$ is transmission line impedance

where

R is the line resistance

X is the line reactance

Using the concept of power flow in the line and analyzing the π-model representation, the power flow at the receiving end of the PSN shown in Figure 3.1 is expressed as

$$S_r = P_r + jQ_r \tag{3.1a}$$

The complex power S, real power, P and reactive power, Q is as shown in the power triangle in Figure 3.2.

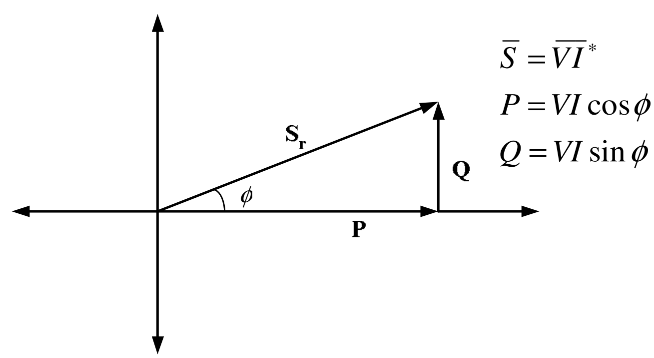

Figure 3.2: The power triangle.

$$S_r = V_r I_r^* \tag{3.1b}$$

where

$$\overline{I_r} = \frac{\overline{V}}{\overline{\overline{Z}}} = \frac{V_S\angle\delta_S - V_r\angle\delta_r}{Z\angle\theta} \tag{3.1c}$$

with $\tan\theta = \frac{X}{R}$ in an impedance triangle.

Using equation (3.1c) in (3.1b) gives

$$S_r = V_r\angle\delta_r\left[\frac{V_S\angle-\delta_S - V_r\angle-\delta_r}{Z\angle-\theta}\right]$$

$$= \frac{V_sV_r\angle(\delta_r - \delta_s) - V_r^2}{Z\angle-\theta}$$

$$= \frac{V_SV_r\angle(\theta+\delta_r-\delta_S)}{Z} - \frac{V_r^2\angle\theta}{Z}$$

$$S_r = \frac{|V_S||V_r|}{|Z|}\angle(\theta + \delta_r - \delta_s) - \frac{|V_r|^2}{|Z|}\angle\theta \tag{3.2}$$

The phasor diagram for the two-bus transmission system of figure 3.1 with the I as the reference phasor.

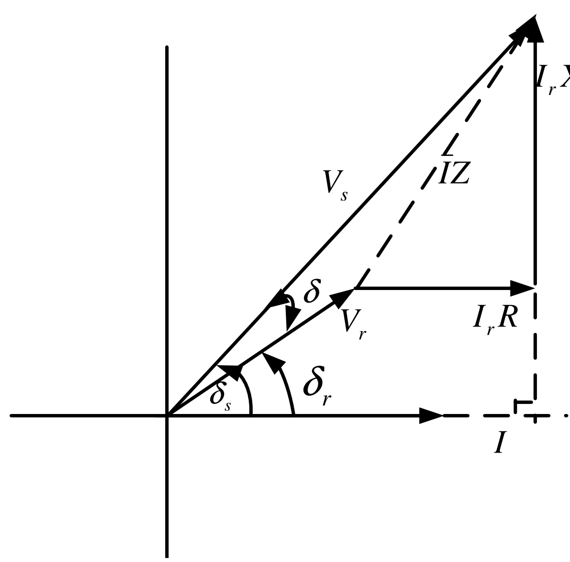

Figure 3.3: The phasor diagram for the two-bus transmission system of figure 3.1.

Expressing S_r in terms of its real and imaginary parts, then (3.1a) equation becomes

$$S_r = \frac{|V_S||V_r|}{|Z|}cos(\theta + \delta_r - \delta_s) + j\frac{|V_S||V_r|}{|Z|}\sin(\theta + \delta_r - \delta_s) - \frac{|V_r|^2}{|Z|}\cos\theta + j\frac{|V_r|^2}{|Z|}\sin\theta \tag{3.3}$$

Rearranging equation (3.3) gives

$$S_r = \frac{|V_S||V_r|}{|Z|} cos(\theta + \delta_r - \delta_s) - \frac{|V_r|^2}{|Z|} \cos\theta + j\left(\frac{|V_S||V_r|}{|Z|} \sin(\theta + \delta_r - \delta_s) - \frac{|V_r|^2}{|Z|} \sin\theta\right) \tag{3.4}$$

But

$$S_r = P_r + jQ_r$$

Then equating real and imaginary parts on both sides, gives

$$P_r = \frac{|V_S||V_r|}{|Z|} cos(\theta - \delta_s + \delta_r) - \frac{|V_r|^2}{|Z|} \cos\theta \tag{3.5}$$

$$Q_r = \frac{|V_S||V_r|}{|Z|} \sin(\theta - \delta_s + \delta_r) - \frac{|V_r|^2}{|Z|} \sin\theta \tag{3.6}$$

Substituting $\delta = \delta_r - \delta_s$ and finding a quadratic equation in terms of Q_r in (3.6) gives

$$\frac{|V_r|^2}{|Z|} \sin\theta - \frac{|V_S||V_r|}{|Z|} \sin(\theta - \delta) + Q_r = 0 \tag{3.7}$$

Therefore, the voltage quadratic equation is given as

$$\frac{\sin\theta}{|Z|} V_r^{\,2} - |V_r| \frac{|V_S| \sin(\theta-\delta)}{|Z|} + Q_r = 0 \tag{3.8}$$

Equation (3.8) is a quadratic equation

Therefore, solving for V_r gives

$$V_r = \frac{\frac{|V_S| \sin(\theta-\delta)}{|Z|} \pm \sqrt{\left(\frac{(|V_S| \sin(\theta-\delta))}{|Z|}\right)^2 - 4\frac{\sin\theta}{|Z|} Q_r}}{2\frac{\sin\theta}{|Z|}} \tag{3.9}$$

For stability, the discriminant of equation (3.9) should be greater than or equal to zero i.e.

$$\frac{(|V_S|^2 \sin^2(\theta-\delta))}{|Z|^2} - 4\frac{\sin\theta}{|Z|} Q_r \geq 0 \tag{3.10}$$

Multiplying both sides with $|Z|^2$, we have

$$|V_s|^2 \sin^2(\theta - \delta) - 4|Z| \sin\theta Q_r \geq 0 \tag{3.11}$$

But the reactance, X from the relevance impedance triangle is given as

$$X = |Z| sin\,\theta$$

Substituting X into equation (3.11), then

$$V_S^2 sin^2(\theta - \delta) - 4XQ_r \geq 0 \tag{3.12}$$

Dividing both sides by $|V_S|^2 sin^2(\theta - \delta)$, then equation (3.12) becomes

$$1 - \frac{4XQ_r}{V_s^2 sin^2(\theta-\delta)} \geq 0 \qquad (3.13)$$

Therefore, the voltage stability index, (Lmn) is obtained as:

$$Lmn = \frac{4XQ_r}{|V_s|^2 sin^2(\theta-\delta)} \leq 1 \qquad (3.14)$$

The FVSI proposed by Musrin and Rahman (2002) hinges on the principle of power flow through a single line for a typical transmission line. It is derived from the voltage quadratic equation at the receiving-end bus of the two-bus system transmission line model shown in Figure 3.1. It is derived from the current flowing in the transmission line to get the voltage quardratic equation. The current, *I* flowing in the network of Fig 3.1 is given as

$$I = \frac{V}{Z} = I_r = \frac{V_s\angle\delta_s - V_r\angle\delta_r}{Z\angle\theta} \qquad (3.15)$$

But power at the receiving end is given by

$$S_r = V_r I_r^*$$

Current at the receiving end is given by

$$I_r = \frac{S_r^*}{V_r^*} = \frac{P_r - jQ_r}{V_r\angle-\delta_r} \qquad (3.16)$$

Using equation (3.15) in (3.16) gives

$$\frac{V_s\angle\delta_s - V_r\angle\delta_r}{R+jX} = \frac{P_r - jQ_r}{V_r\angle-\delta_r} \qquad (3.17)$$

Therefore,

$$V_r\angle-\delta_r V_s\angle\delta_s - V_r^2 = (R+jX)(P_r - jQ_r)$$

$$V_r V_s\angle(\delta_s - \delta_r) - V_r^2 = (R+jX)(P_r - jQ_r)$$

$$V_r V_s\angle(\delta_s - \delta_r) - V_r^2 = RP_r + XQ_r + j(XP_r - RQ_r) \qquad (3.18)$$

Rectangular form of equation (3.18) is obtained as

$$V_r V_s \cos(\delta_s - \delta_r) - V_r^2 + jV_r V_s \sin(\delta_s - \delta_r) = RP_r + XQ_r + j(XP_r - RQ_r) \qquad (3.19)$$

Equating Real and Imaginary parts on both sides of equation (3.19), gives

$$V_r V_s \cos(\delta_s - \delta_r) - V_r^2 = RP_r + XQ_r \qquad (3.20)$$

$$V_r V_s \sin(\delta_s - \delta_r) = XP_r - RQ_r \qquad (3.21)$$

Making P_r the subject in equation (3.21) yields

$$P_r = \frac{RQ_r + V_r V_s \sin(\delta_s - \delta_r)}{X} \qquad (3.22)$$

Substituting equation (3.22) into equation (3.20) and re-arranging yields

$$V_r V_s \cos(\delta_s - \delta_r) - V_r^2 = \frac{R}{X}[RQ_r + V_r V_s \sin(\delta_s - \delta_r)] + XQ_r \tag{3.23}$$

$$= \frac{R^2 Q_r}{X} + \frac{V_r V_s R \sin(\delta_s - \delta_r)}{X} + XQ_r$$

$$V_r^2 + V_r\left[\frac{V_s R \sin(\delta_s - \delta_r)}{X} - V_s \cos(\delta_s - \delta_r)\right] + \frac{R^2 Q_r}{X} + XQ_r = 0$$

Therefore,

$$V_r^2 + V_r\left[\frac{V_s R \sin(\delta_s - \delta_r)}{X} - V_s \cos(\delta_s - \delta_r)\right] + Q_r\left(\frac{R^2}{X} + X\right) = 0 \tag{3.24}$$

Now, solving the quadratic equation (3.24) in V_r gives

$$V_r = \frac{V_s \cos(\delta_s - \delta_r) - \frac{V_s R \sin(\delta_s - \delta_r)}{X} \pm \sqrt{\left[\frac{V_s R \sin(\delta_s - \delta_r)}{X} - V_s \cos(\delta_s - \delta_r)\right]^2 - 4Q_r\left(\frac{R^2}{X} + X\right)}}{2} \tag{3.25}$$

For the value of V_r to be real and positive, then the discriminant of equation (3.25) must be greater than or equal to zero. Thus:

$$\left(\frac{V_s R \sin(\delta_s - \delta_r)}{X} - V_s \cos(\delta_s - \delta_r)\right)^2 - 4Q_r\left(\frac{R^2}{X} + X\right) \geq 0 \tag{3.26}$$

$$\frac{(V_s R \sin(\delta_s - \delta_r) - XV_s \cos(\delta_s - \delta_r))^2}{X^2} - 4Q_r\left(\frac{R^2}{X} + X\right) \geq 0 \tag{3.27}$$

$$(V_s R \sin(\delta_s - \delta_r) - XV_s \cos(\delta_s - \delta_r))^2 - 4X^2 Q_r \frac{(R^2 + X^2)}{X} \geq 0 \tag{3.28}$$

Substitute for $Z^2 = R^2 + X^2$ in equation (3.28)

$$(V_s R \sin(\delta_s - \delta_r) - XV_s \cos(\delta_s - \delta_r))^2 - 4XQ_r(Z^2) \geq 0 \tag{3.29}$$

$$4XQ_r(Z^2) \leq (V_s R \sin(\delta_s - \delta_r) - XV_s \cos(\delta_s - \delta_r))^2 \tag{3.30}$$

Dividing both sides of equation (3.30) by $\left(V_s R \sin\left(\delta_s - \delta_r\right) - XV_s \cos\left(\delta_s - \delta_r\right)\right)^2$, gives

$$\frac{4XQ_r(Z^2)}{(V_s R \sin(\delta_s - \delta_r) - XV_s \cos(\delta_s - \delta_r))^2} \leq 1 \tag{3.31}$$

Letting $\delta = \delta_s - \delta_r$, then

$$\frac{4XQ_r(Z^2)}{(V_s R \sin\delta - XV_s \cos\delta)^2} \leq 1 \tag{3.32}$$

Assuming the angle difference δ is very small i.e. If $\delta \to 0$ then $\sin\delta \to 0$ and $\cos\delta \to 1$, hence,

$$\frac{4XQ_rZ^2}{X^2V_S^2} \leq 1 \tag{3.33}$$

Therefore the Fast Voltage Stability Index (FVSI), is given as

$$FVSI = \frac{4Q_rZ^2}{XV_S^2} \leq 1 \tag{3.34}$$

The FVSI can be explicitly derived from Lmn when the voltage angle difference 'δ', (the difference between the voltage angles of the sending and receiving ends) is assumed to be very small.

From the expression of the Lmn index in equation (3.14), when $\delta \approx 0$, it can be inferred that:

$$Lmn = \frac{4XQ_r}{|V_s|^2 sin^2(\theta - o)} \leq 1$$

$$= \frac{4XQ_r}{\left|V_s\right|^2 (\sin\theta)^2} \leq 1 \tag{3.35}$$

Recall from the impedance triangle that

$$X = |Z| sin\,\theta$$

which implies

$$sin\theta = \frac{X}{|Z|}. \tag{3.36}$$

Substituting equation (3.36) into equation (3.35) and simplifying yields

$$\frac{4Q_r(|Z|)^2}{|V_S|^2 X} \leq 1 \tag{3.37}$$

which is equivalent to the expression of FVSI given in equation (3.34).

We therefore propose to combine equations (3.14) and (3.37) into a single equation to compute the proximity to voltage collapse according to a switching function, σ, as shown in equation (3.38). Each value of δ computed from the load-flow program is tested against a threshold value, δ_c, in order to determine whether σ is 1 or 0.

The corollary is combining equations (3.14) and (3.37) into one equation to yield a new stability index that gain fastness and accuracy with improved stability. This is given as:

$$NLSI\_1 = \frac{4Q_r}{|V_S|^2}\left[\frac{(|Z|)^2}{X}\sigma - \frac{X}{\sin^2(\theta - \delta)}(\sigma - 1)\right] \leq 1 \qquad \sigma = \begin{cases} 1 & \delta < \delta_c \\ 0 & \delta \geq \delta_c \end{cases} \tag{3.38}$$

Note that δ is used here as a modifier.

where 'σ' is a switching function whose value depends on whether the angle difference, δ, is very small or not. A large voltage angle difference between two load buses indicates a heavily loaded power system network with large power flows or increased impedance between the load buses. Dobson *et al.,* (2010) reported that in a simulation of the grid carried out before the August 2003, Northeastern blackout showed increasing angle differences between Cleveland and West Michigan, revealing that large angle differences could be a risk signal to the occurrence of blackout or system collapse (Dobson *et al.,* 2010). Therefore, the voltage angle difference, delta '**δ**' cannot be totally ignored as done in the mathematical formulation of FVSI. When NLSI_1 is less than 1, the system is stable. The closer its value approaches one (1), then system is unstable and near voltage collapsed.

3.2.2 Determination of the Switching Function for the NLSI_1

The switching function σ, is dependent on the voltage angle difference, δ. Therefore, to determine the point at which switching will take place, a study of the error percentage of the voltage stability indices with reference to the voltage angle difference, δ is considered. The base case results of the Lmn and FVSI are used. Error can be defined as the mathematical difference between the true value of a mathematical quantity and a calculated or measured value. The error percentage is considered using the two techniques of specifying errors i.e. the absolute error of an approximation and the relative error of the approximation. The absolute error gives how large the error is, and the relative error gives how large the error is relative to the correct value (Donna, 2012). The absolute error, relative error, and percent error are mathematically represented as

Absolute error, $E_{abs} = | D_{base} - D_{used}|$ (3.39)

Relative error, $E_{rel} = | (D_{base} - D_{used}) / D_{base} |$ (for $D_{base} \neq 0$) (3.40)

Percent error, $\% E = | (D_{base} - D_{used}) / D_{base} | \times 100$ (for $D_{base} \neq 0$) (3.41)

where

D_{base} is the base value,

D_{used} is the value used

The Lmn is taken as the base value, i.e. D_{base}. More so that it is considered to be the true representation of the voltage stability index and the most accurate among them all while the FVSI is an approximation of Lmn and it is the value used, D_{used}. It is important to note that the switching point is unique to individual power system networks.

3.3 Power Flow Analysis

Power-flow studies are carried out to generate the data used for the calculation of the voltage stability indices for both the base case and the contingency analysis of the two selected case studies in this thesis using a power flow code in MATLAB environment.

Power flow analysis plays a very important role in power system planning, control and operation to ensure that power systems are operated efficiently (Kundur, 1994). It is very crucial for all calculations relating to the network since it concerns the network performance in its steady-state operating conditions. Since load-flow is a non-linear problem, it must be solved iteratively hence the use of any of the following methods: the Gauss-Siedel, Newton-Raphson, and fast decoupled methods (Saadat, 2004).

The Newton-Raphson method (NR) is used in this research work because of its faster convergence that makes it to find its relevance in large power systems. The number of iterations required to obtain a solution is not dependent on the size of the network. In addition, the Newton-Raphson method is well suited for software computations. Simply stated, it has a very high convergence speed compared to other iterative solution methods and its convergence criteria are specified to ensure convergence for bus real power and reactive power mismatches which give direct control of the accuracy specified for the load flow solution (Saadat, 2004; Afolabi *et al.,* 2015). The power flow equation is formulated in polar form due to the fact that in the power flow problem, real power and voltage magnitude are specified for the voltage-controlled buses (Samuel *et al.,* 2014 (b); Adebayo *et al.,* 2014).

The system nodal (n-bus) equations are given as

$$I_i = \sum_{j=1}^{n} Y_{ij}V_i \tag{3.42}$$

In polar form, equation (3.42) is recast as

$$I_i = \sum_{j=1}^{n} |Y_{ij}||V_i|\angle(\theta_{ij} + \delta_j) \tag{3.43}$$

But complex power at bus i is

$$P_i - jQ_i = V^* I_i \tag{3.44}$$

i.e $$P_i - jQ_i = |V_i|\angle(-\delta i)\sum_{j=1}^{n} |Y_{ij}||V_i|\angle(\theta_{ij} + \delta_j) \tag{3.45}$$

Separating the real and the imaginary parts, we have

$$P_i = \sum_{j=1}^{n} |Y_{ij}||V_i||V_j|\cos(\theta_{ij} - \delta_i + \delta_j) \tag{3.46}$$

$$Q_i = -\sum_{j=1}^{n} |Y_{ij}||V_i||V_j|sin(\theta_{ij} - \delta_i + \delta_j) \tag{3.47}$$

Expanding equations (3.46) and (3.47) in a Taylor series, results in a set of linear equations involving a Jacobian matrix which gives the linear relationship between small changes in voltage angle with small changes in real power as well as small changes in magnitude of voltage with small changes in reactive power. i.e.

$$\begin{bmatrix} \Delta P_2^{(k)} \\ \vdots \\ \Delta P_n^{(k)} \\ \hline \Delta Q_2^{(k)} \\ \vdots \\ \Delta Q_n^{(k)} \end{bmatrix} = \left[\begin{array}{ccc|ccc} \frac{\partial P_2}{\partial \delta_2}^{(k)} & \cdots & \frac{\partial P_2}{\partial \delta_n}^{(k)} & \frac{\partial P_2}{\partial |V_2|}^{(k)} & \cdots & \frac{\partial P_2}{\partial |V_n|}^{(k)} \\ \vdots & \ddots & \vdots & \vdots & \ddots & \vdots \\ \frac{\partial P_n}{\partial \delta_2}^{(k)} & \cdots & \frac{\partial P_n}{\partial \delta_n}^{(k)} & \frac{\partial P_n}{\partial |V_2|}^{(k)} & \cdots & \frac{\partial P_n}{\partial |V_n|}^{(k)} \\ \hline \frac{\partial Q_2}{\partial \delta_2}^{(k)} & \cdots & \frac{\partial Q_2}{\partial \delta_n}^{(k)} & \frac{\partial Q_2}{\partial |V_2|}^{(k)} & \cdots & \frac{\partial Q_2}{\partial |V_n|}^{(k)} \\ \vdots & \ddots & \vdots & \vdots & \ddots & \vdots \\ \frac{\partial Q_n}{\partial \delta_2}^{(k)} & \cdots & \frac{\partial Q_n}{\partial \delta_n}^{(k)} & \frac{\partial Q_n}{\partial |V_2|}^{(k)} & \cdots & \frac{\partial Q_n}{\partial |V_n|}^{(k)} \end{array}\right] \begin{bmatrix} \Delta \delta_2^{(k)} \\ \vdots \\ \Delta \delta_n^{(k)} \\ \hline \Delta |V_2^{(k)}| \\ \vdots \\ \Delta |V_n^{(k)}| \end{bmatrix} \tag{3.48}$$

This can be rewritten in a short form as

$$\begin{bmatrix} \Delta P \\ \Delta Q \end{bmatrix} = \begin{bmatrix} J1 & J2 \\ J3 & J4 \end{bmatrix} \begin{bmatrix} \Delta \delta \\ |\Delta V| \end{bmatrix} \tag{3.49}$$

ΔP and ΔQ represent differences between specified values and calculated values respectively, ΔV and Δδ represent voltage magnitude and voltage angle respectively in incremental forms and sub-matrices J1 through J4 form the Jacobian matrix (Saadat, 2004; Nayak and Wadhwani, 2014).

The scheduled and the calculated values of the power residuals of the term $\Delta P_i^{(k)}$ and $\Delta Q_i^{(k)}$ are given as

$$\Delta P_i^{(k)} = P_i^{sch} - P_i^{(k)} \tag{3.50}$$

$$\Delta Q_i^{(k)} = Q_i^{sch} - Q_i^{(k)} \tag{3.51}$$

The new estimates for the voltage angles and magnitudes are respectively given as

$$\delta_i^{(k+1)} = \delta_i^{(k)} + \Delta\delta_i^{(k)} \tag{3.52}$$

$$\left|V_i^{(k+1)}\right| = \left|V_i^{(k)}\right| + \Delta\left|V_i^{(k)}\right| \tag{3.53}$$

The calculation is repeated until

$$\left|\Delta P_i^{(k)}\right| \leq \in \tag{3.54}$$

$$\left|\Delta Q_i^{(k)}\right| \leq \in \tag{3.55}$$

where $\in$ is a very small number around 1.0 X 10^{-6}.

3.3.1. Classification of power system buses

In power-flow analysis, power system buses are classified into three major bus types (Saadat, 2004). These are as follows:

1. Slack bus is also known as swing bus or reference bus. This is where the magnitude and phase angle of the voltage are specified. This bus generates or absorbs the excess power required to balance the active powers throughout the network. Slack bus is one of the generator buses in the power system network.
2. Load buses are buses whose active and reactive powers are specified. The magnitudes and the phase angles of the bus voltages are unknown. They are also referred to as P-Q buses.
3. Generator buses: These are also known as voltage-controlled buses. At these buses, the real powers (P) and voltage magnitudes (V) are specified. The

phase angles of the voltages and the reactive powers are to be determined. The limits on the value of the reactive power are also specified. These buses are also called P-V buses (Saadat, 2004; Dharamji and Tanti, 2012). This classification is as depicted in Table 3.1.

Table: 3.1: Bus Classification

Bus Identity	Known Quantities	Quantities to be specified
Slack Bus	$\lvert\overline{V}\rvert$, δ	P,Q
Load Bus	P,Q	$\lvert\overline{V}\rvert$, δ
Generator Bus	P, $\lvert\overline{V}\rvert$	Q, δ

3.3.2 Power-flow Algorithm using Newton Raphson Method

1. Load buses (P, Q specified), flat voltage start. For voltage controlled buses (P, $\lvert\overline{V}\rvert$ specified), δ is set equal to zero (0).

2. Load buses, $\boldsymbol{P_i^{(k)}}$ and $\boldsymbol{Q_i^{(k)}}$ are calculated and $\boldsymbol{\Delta P_i^{(k)}}$ and $\boldsymbol{\Delta Q_i^{(k)}}$ are calculated.

3. For voltage controlled buses, $\boldsymbol{P_i^{(k)}}$ and $\boldsymbol{\Delta P_i^{(k)}}$ are calculated

4. The elements of the Jacobian matrix are calculated.

5. The linear simultaneous equations are solved directly by triangle factorization and Gaussian elimination.

6. The new voltage magnitudes and phase angles are computed.

7. The process is continued until the residuals $\Delta\boldsymbol{P_i^{(k)}}$ and $\Delta\boldsymbol{Q_i^{(k)}}$ are less than the specified accuracy.

3.3.3 Power flow in MATLAB environment

In order to carry out the power flow analysis for the case studies using the Newton-Raphson method in the MATLAB environment, the following variables are normally specified:

a) power system base MVA- The value used is Base MVA = 100
b) power mismatch accuracy
c) acceleration factor: The value used = 0.001
d) maximum number of iterations. The value used is maxiter = 100
e) Bus classified as one (1) for slack bus, zero (0) for load buses and two (2) for generator bus.

The power flow simulation was done using the MATLAB R2012a software. The MATLAB programme of the Newton-Raphson method of power flow solution that has been developed for the practical system (Saadat, 2002) is used based on the following developed files:

a) bus data file
b) line data file
c) ifybus
d) newtonrap
e) busout
f) lineflow

This program was further extended to cater for the extraction of data from the above mentioned files to calculate the voltage stability indices for analysis and prediction. These file are

g) Fvsi_index_1
h) Lmn_index_1
i) NLSI_1_index_IEEE14
j) NLSI_1_index_NNG28

Flow chart for power flow study using the Newton-Raphson iterative method and voltage stability indices calculation is as shown in Figure 3.4

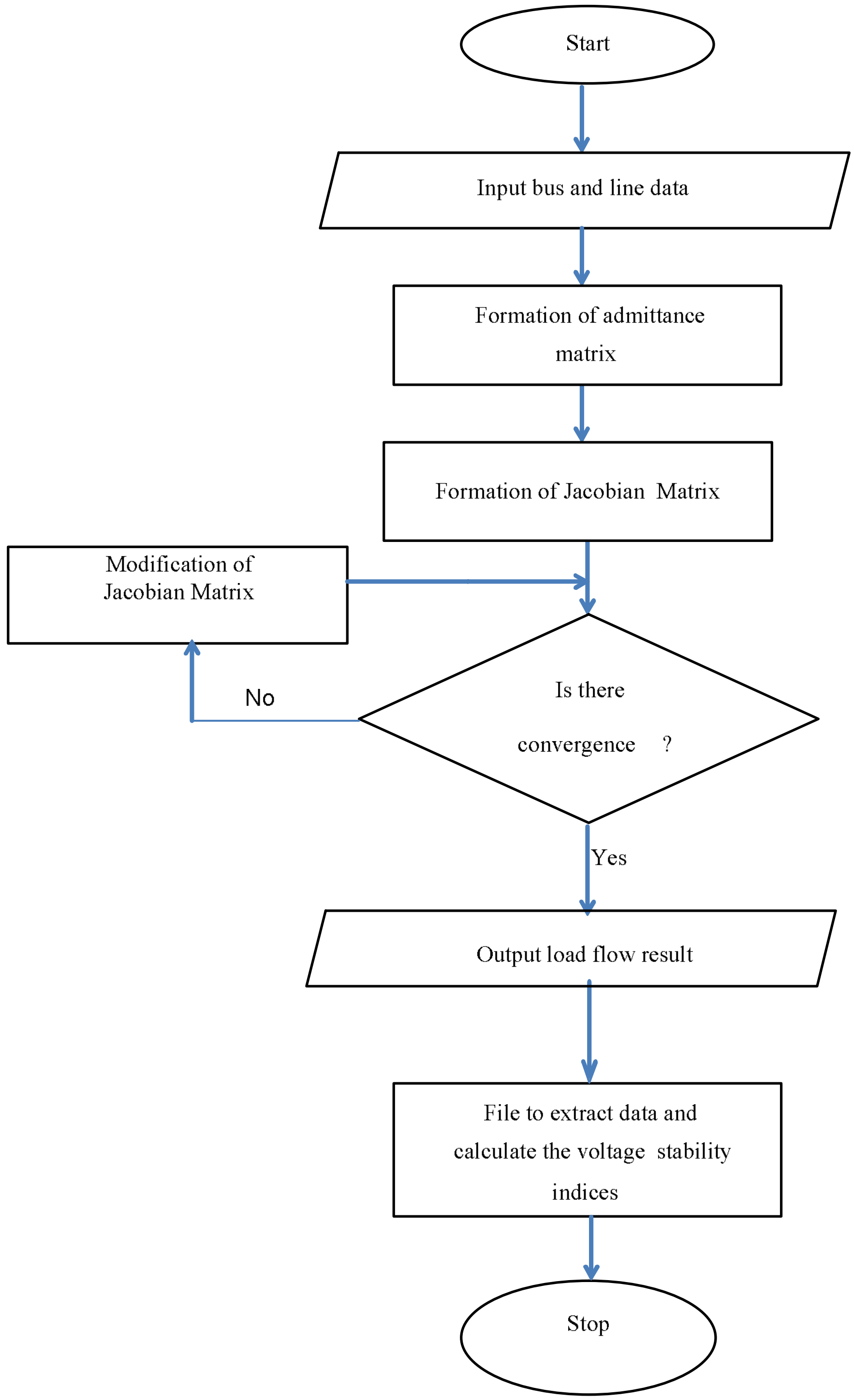

Figure 3.4 Flow chart showing power flow study using the Newton Raphson Iterative Method

3.4 Determination of the Load-Ability and Identification of Weak Bus

The prediction of voltage collapse is encapsulated in the determination of the maximum load-ability, identification of the weakest bus of the network and the critical line with respect to load buses. This information is useful to optimally locate possible points of placement of compensation devices to mitigate against voltage collapse in the PSNs. The following algorithm steps are followed in determining the maximum loadability and weak bus identification:

1. Input the bus and the line data for the IEEE 14-bus test system and NNG 330-kV, 28-bus network.
2. The Power flow solution program is run for the base case using the Newton-Raphson method in the MATLAB environment.
3. The line stability indices'(Lmn, FVSI and NLSI_1) values are calculated for the base case for all the lines of IEEE 14-bus system and NNG 330-kV, 28-bus network.
4. A load bus (PQ Bus) is selected and from the base case its reactive power demand is gradually increased while keeping the loads on the other buses at the base load until the stability index value approaches one (1).
5. The value of the line stability index for each variation in the load is calculated.
6. The line with the greatest line stability index value is the most critical line of the bus.
7. Then another load bus (PQ bus) is selected and steps 1-5 are repeated.
8. The maximum reactive power loading is extracted and is termed "the maximum loadability" of the selected load bus obtained from step 4.
9. The voltage at the critical loading is obtained. This is known as the critical voltage of that particular load bus.

The maximum load-ability is ranked the highest implying the weakest bus in the system. This is a possible location of compensation device for voltage stability enhancement. Figure 3.5 shows the flow chart for calculating the voltage stability indices being considered in this work.

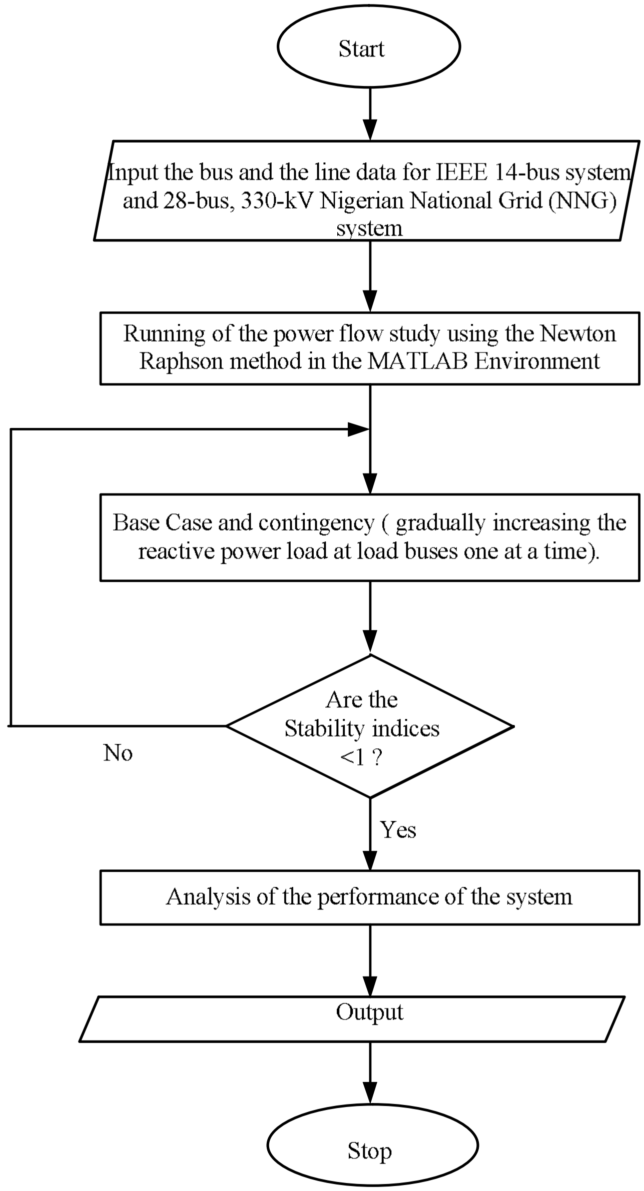

Figure 3.5: Steps for calculating the voltage stability indices

3.5 Description of the Case Studies

The case studies used in this work are the IEEE 14-bus test network for validation of the index and a practical power system network, the Nigerian National Grid, 330-kV, 28-bus network.

3.5.1 The IEEE 14-Bus Test System

The IEEE 14-bus test system has 5 generator buses (PV), 9 load buses (PQ) and 20 interconnected lines or branches. Out of the generator buses, bus 1 is selected as the slack bus. Figure 3.6 shows the single-line diagram of the system. The bus and line data used for the power flow analysis are as presented.

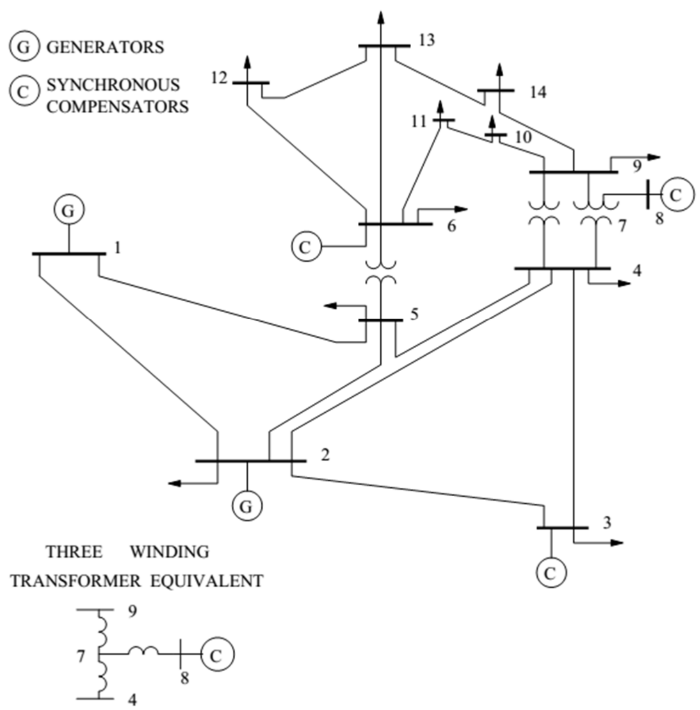

Figure 3.6: Single-line diagram of the 14-Bus IEEE System (Kodsi and Canizares, 2003)

The bus and line data used are as presented in Tables 3.2 and 3.3, respectively. The bus codes identification used in the MATLAB simulation are: 0 (zero) for load bus, 1 for slack bus and 2 for voltage bus.

Table 3.2: Bus data of IEEE 14-BUS Test System

			Angle	Load		Generator				Static MVAr
Bus No.	Bus Code	Vmag	Degree	MW	MVAr	MW	MVAr	Qmin	Qmax	+Qc/-Ql
1	1	1.06	0	0	0	0	0	0	0	0
2	2	1.045	0	21.7	12.7	0	42.4	-40	50	0
3	2	1.01	0	94.2	19	0	0	0	40	0
4	0	1	0	47.8	-3.9	0	0	0	0	0
5	0	1	0	7.6	1.6	0	0	0	0	0
6	2	1	0	11.2	7.5	0	0	-6	24	0
7	0	1	0	0	0	0	0	0	0	0
8	2	1	0	0	0	0	0	-6	24	0
9	0	1	0	29.5	16.6	0	0	0	0	0
10	0	1	0	9	5.8	0	0	0	0	0
11	0	1	0	3.5	1.8	0	0	0	0	0
12	0	1	0	6.1	1.6	0	0	0	0	0
13	0	1	0	13.5	5.8	0	0	0	0	0
14	0	1	0	14.9	5	0	0	0	0	0

Source: Kodsi and Canizares, 2003

Table 3.3: Line data of IEEE 14-Bus Test System

Line No	Bus		Line impedance		Susceptance
	From Bus	To Bus	R (p.u.)	X (p.u.)	1/2 B (p.u)
1	1	2	0.1938	0.05917	0.0264
2	1	5	0.054	0.22304	0.0219
3	2	3	0.047	0.19797	0.0187
4	2	4	0.0581	0.17632	0.0246
5	2	5	0.057	0.17388	0.017
6	3	4	0.067	0.17103	0.0173
7	4	5	0.0134	0.04211	0.0064
8	4	7	0	0.20912	0
9	4	9	0	0.55618	0
10	5	6	0	0.25202	0
11	6	11	0.095	0.1989	0
12	6	12	0.1229	0.25581	0
13	6	13	0.0662	0.13027	0
14	7	8	0	0.17615	0
15	7	9	0	0.11001	0
16	9	10	0.0318	0.0845	0
17	9	14	0.1271	0.27038	0
18	10	11	0.0821	0.19207	0
19	12	13	0.2209	0.19988	0
20	13	14	0.1709	0.34802	0

Source: Kodsi and Canizares, 2003

3.5.2 The NNG 330-kV, 28-Bus Network

The present installed capacity of the Nigerian National Grid (NNG) is about 6,000MW, out of which about 67 percent is thermal and the balance is hydro-based. Presently, the

NNG has 5,000km of 330-kV lines. The 330-kV lines feed 23 substations employing transformers with voltage rating of 330/132-kV and a combined capacity of 4,800 MVA at a utilization factor of 80%. The system frequency is 50Hz. The network has a wheeling capacity less than 4,000 MW (Samuel *et al.*, 2012). The NNG is characterized by poor voltage profile in most parts of the network, especially in the Northern part of the country due to inadequate dispatch and control infrastructures (Adebayo *et al.*, 2014). The grid is radial, fragile and overloaded hence high transmission losses and frequent system collapse being experienced (Nigeria Electricity Regulatory Commission, 2005). All these make the NNG highly stressed, weak and prone to voltage instability and eventually voltage collapse (Onohaebi and Apeh, 2007; Samuel, *et al.*, 2014). The single-line diagram of NNG, 330-kV, 28-Bus Network is shown in Figure 3.7. It has 9 generator buses (PV), 19 Load buses (PQ) and 31 interconnected lines or branches.

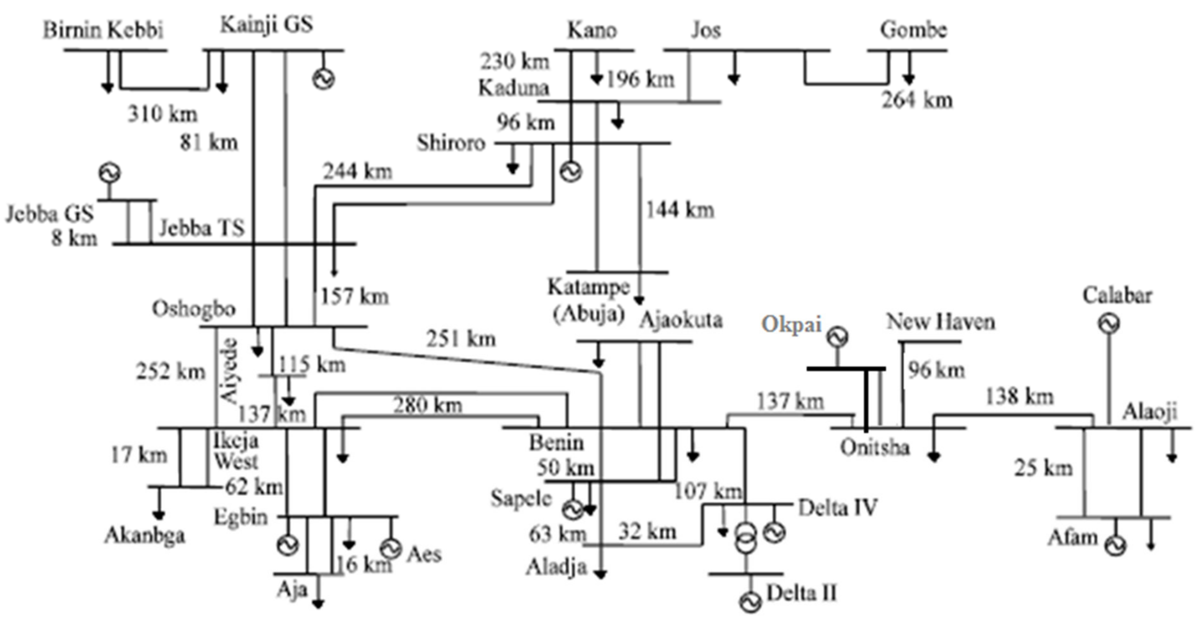

Figure 3.7: The NNG 330-kV, 28-Bus Network diagram (Oleka *et al.*, 2016; TCN, 2015).

The bus data of NNG 330-kV, 28-bus network is as presented in Table 3.4 and the transmission line data are also presented in Table 3.5

Table 3.4: Bus Data of NNG 330-kV, 28-Bus Network

Bus. No.	Bus Name	Bus Code	Voltage Mag. Pu	Angle Degree	Load		Generation	
					MW	MVAr	MW	MVAr
1	Egbin	1	1.05	0	68.9	51.7	251.538	641.299
2	Delta	2	1.05	15.424	0	0	670	82.628
3	Aja	0	1.04	-0.57	274.4	205.8	0	0
4	Akangba	0	0.97	0.482	344.7	258.5	0	0
5	Ikeja West	0	0.986	1.408	633.2	474.9	0	0
6	Ajaokuta	0	1.026	8.739	13.8	10.3	0	0
7	Aladja	0	1.046	14.04	96.5	72.4	0	0
8	Benin	0	1.011	9.306	383.4	287.5	0	0
9	Ayede	0	0.932	2.335	275.8	206.8	0	0
10	Osogbo	0	0.966	8.642	201.2	150.9	0	0
11	Afam	2	1.05	13.273	52.5	39.4	431	590.551
12	Alaoji	0	1.007	12.057	427	320.2	0	0
13	New Haven	0	0.905	3.322	177.9	133.4	0	0
14	Onitsha	0	0.949	6.268	184.6	138.4	0	0
15	Birnin-Kebbi	0	1.01	26.299	114.5	85.9	0	0
16	Gombe	0	0.844	4.905	130.6	97.9	0	0
17	Jebba	0	1.046	25.523	11	8.2	0	0
18	Jebba-GS	2	1.05	26.022	0	0	495	159.231
19	Jos	0	0.93	12.901	70.3	52.7	0	0
20	Kaduna	0	0.951	8.791	193	144.7	0	0
21	Kainji	2	1.05	31.819	7.5	5.2	624.7	-65.319
22	Kano	0	0.818	-1.562	220.6	142.9	0	0
23	Shiroro	2	1.05	13.479	70.3	36.1	388.9	508.034
24	Sapele	2	1.05	12.015	20.6	15.4	190.3	283.405
25	Calabar	0	0.951	21.703	110	89	0	0
26	Katampe	0	1	9.242	290.1	145	0	0
27	Okpai	2	1.05	46.869	0	0	750	193.093
28	AES-GS	2	1.05	5.871	0	0	750	488.128

Source: TCN, 2015

Table 3.5: Line Data of NNG 330-kV, 28-Bus Network

L/ No.	From Bus	B/Name	To B/No.	B/Name	R (pu)	X (pu)	Susceptance B(pu)
1	3	Aja	1	Egbin	0.00066	0.00446	0.06627
2	4	Akangba	5	Ikeja west	0.0007	0.00518	0.06494
3	1	Egbin	5	Ikeja west	0.00254	0.01728	0.25680
4	5	Ikeja west	8	Benin	0.01100	0.08280	0.40572
5	5	Ikeja west	9	Ayede	0.00540	0.04050	
6	5	Ikeja west	10	Osogbo	0.01033	0.07682	0.96261
7	6	Ajaokuta	8	Benin	0.00799	0.05434	0.80769
8	2	Delta	8	Benin	0.00438	0.03261	0.40572
9	2	Delta	7	Aladja	0.00123	0.00914	0.1146
10	7	Aladja	24	Sapele	0.00258	0.01920	0.24065
11	8	Benin	14	Onitsha	0.00561	0.04176	0.52332
12	8	Benin	10	Osogbo	0.01029	0.07651	0.95879
13	8	Benin	24	Sapele	0.00205	0.01393	0.2071
14	9	Ayede	10	Osogbo	0.00471	0.03506	0.43928
15	15	Birnin K	21	Kanji	0.01271	0.09450	1.18416
16	10	Osogbo	17	Jebb TS	0.00643	0.04786	0.59972
17	11	AFAM	12	Alaoji	0.00102	0.00697	0.10355
18	12	Alaoji	14	Onitsha	0.00566	0.04207	0.52714
19	13	New Haven	14	Onitsha	0.00393	0.02926	0.36671
20	16	Gombe	19	Jos	0.01082	0.08048	1.00844
21	17	Jebb TS	18	Jebb GS	0.00033	0.00223	0.03314
22	17	Jebb TS	23	Shiroro	0.01000	0.07438	0.93205
23	17	Jebb TS	21	Kanji	0.00332	0.02469	0.30941
24	19	Jos	20	Kaduna	0.00803	0.05975	0.74869
25	20	Kaduna	22	Kano	0.00943	0.07011	0.87857
26	20	Kaduna	23	Shiroro	0.00393	0.02926	0.36671
27	23	Shiroro	26	Katempe	0.00614	0.04180	0.6213
28	12	Alaoji	25	Calabar	0.0071	0.0532	0.38
29	14	Onitsha	27	Okpai	0.00213	0.01449	0.21538
30	25	Calabar	27	Okpai	0.0079	0.0591	0.39000
31	5	Ikeja west	28	AES GS	0.00160	0.01180	0.09320

Source: TCN, 2015

3.6 Summary

This chapter presented the derivation of the proposed new line stability index (NLSI_1). The transmission line whose stability index is one (1) is said to be unstable and when it is one (1), it simply means there will be voltage collapse. The stability indices are able to reveal the weakest line and they can test for maximum load-ability which brings out the weakest bus in the PSN. The indices were calculated based on data from Newton-Raphson power-flow solution to predict proximity to voltage collapse in a given PSN. The determination of the switching function is also presented. As a background review of methods, power flow analysis is presented in section 3.4. The PSNs data for simulations of the power flow solution required to generate data for the base case and contingencies simulations were also presented.

CHAPTER FOUR

RESULTS AND DISCUSSIONS

4.1 Introduction

In chapter three material and methods were presented and the new line stability index, NLSI_1 for predicting voltage collapse situations in a power system was derived. This chapter presents case study comparisons of the new index to the existing indices **Lmn** and **FVSI** so as to validate the new index, **NLSI_1**. The simulations are carried out for the two PSNs used as case studies and the results are discussed.

4.2 Simulations

Simulations are carried out based on the following two scenarios:

i. The base case: This is the normal operational mode.

ii. The contingency: This is the variation of the reactive power for load buses from the base case one at a time.

These two scenarios are carried out on two case studies: the IEEE 14-bus test system and the NNG 330-kV, 28-bus network.

4.2.1 Simulation Results of the IEEE 14-bus test system

The power flow simulation was performed on the IEEE 14-bus test system network for the base case and the stability indices were calculated for validation of voltage stability indices (as shown in Appendix A). The power flow solution using the Newton-Raphson method is as shown in Table 4.1. Figure 4.2 shows the graph of voltage magnitude versus bus number (voltage profile).

Table 4.1: Power Flow solution for the IEEE 14-bus System by NR Method

Bus	Voltage	Angle	Load		Generation		Injected
No.	Mag.	Degree	MW	MVAr	MW	MVAr	MVAr
1	1.06	0	0	0	275.194	-1.495	0
2	1.035	-6.056	21.7	12.7	0	42.161	0
3	1.01	-13.993	94.2	19	0	39.906	0
4	1.001	-11.13	47.8	-3.9	0	0	0
5	1.007	-9.543	7.6	1.6	0	0	0
6	0.99	-15.93	11.2	7.5	0	20.312	0
7	0.983	-14.576	0	0	0	0	0
8	1	-14.576	0	0	0	9.594	0
9	0.965	-16.455	29.5	16.6	0	0	0
10	0.961	-16.696	9	5.8	0	0	0
11	0.972	-16.459	3.5	1.8	0	0	0
12	0.973	-16.918	6.1	1.6	0	0	0
13	0.967	-16.981	13.5	5.8	0	0	0
14	0.946	-17.877	14.9	5	0	0	0

In Figure 4.1, it is observed that bus 14 has a voltage magnitude of 0.946 p.u. This is the only bus whose voltage falls short of the ±5% tolerance margin of the voltage criterion.

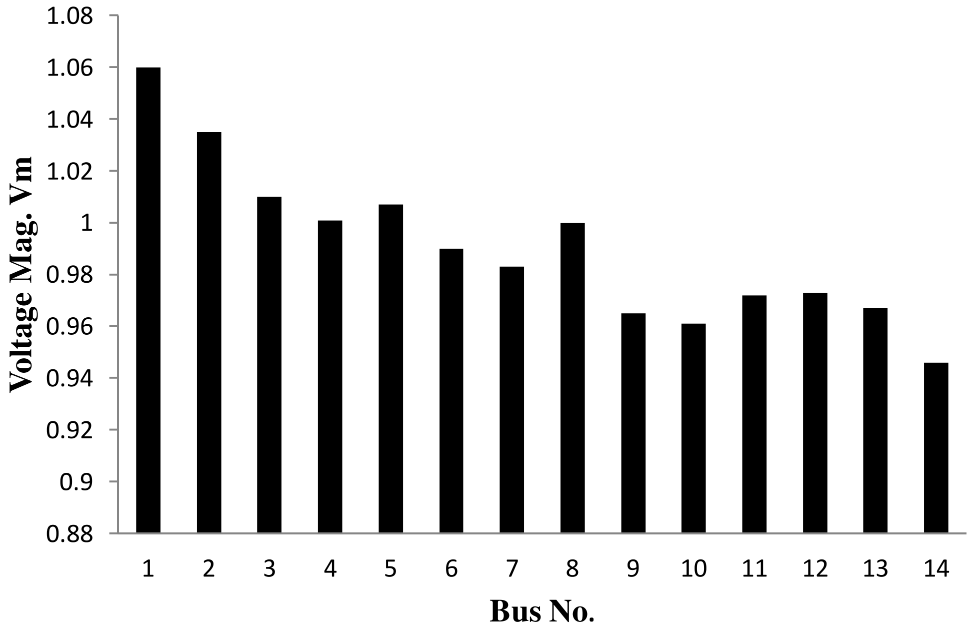

Figure 4.1: The bar chart of voltage profiles for the IEEE 14-Bus System

4.2.1.1 Determination of the Switching Function for IEEE 14-bus System

Determination of the switching function for IEEE 14-bus system is carried out by using a test base case simulation of the Lmn and FVSI stability indices in line with the concept outlined in section 3.3. The switching function is unique to each network and is decided, based on the percentage error between the two stability indices and therefore the error so considered should be reasonably small. The simulation result of the test base case to determine the switching function for IEEE 14-bus system is as shown in Table 4.2.

Table 4.2: Determination of the switching for IEEE 14-bus system

Line	From	To	Lmn	FVSI	Error %	$\delta = \delta_1 - \delta_2$
2	1	5	0.08971	0.08029	10.5005	9.543
3	2	3	0.01043	0.00957	8.245446	7.937
1	1	2	0.02795	0.02575	7.871199	6.056
4	2	4	0.01739	0.01626	6.497987	5.074
5	2	5	0.02699	0.02583	4.297888	3.487
6	3	4	0.1024	0.10618	3.691406	-2.863
17	9	14	0.03355	0.03275	2.384501	1.422
13	6	13	0.05731	0.05623	1.884488	1.051
12	6	12	0.0368	0.03618	1.684783	0.988
7	4	5	0.01086	0.01104	1.657459	-1.587
20	13	14	0.05856	0.05765	1.553962	0.896
10	5	6	0.09208	0.09094	1.238054	6.387
11	6	11	0.05762	0.05711	0.885109	0.529
9	4	9	0.16108	0.15969	0.862925	5.325
8	4	7	0.0773	0.07702	0.362225	3.446
18	10	11	0.03628	0.03641	0.358324	-0.237
16	9	10	0.00885	0.00882	0.338983	0.241
19	12	13	0.01944	0.01939	0.257202	0.063
15	7	9	0.07662	0.07654	0.104411	1.879
14	7	8	0.06882	0.06882	0	0

*Yellow shows the switching point.

The index, Lmn is more accurate than the FVSI index, hence it is chosen as the base value in the determination of the percentage error. The switching function σ, chosen has percentage error of 2.384 corresponding to angle difference, δ, of 1.422. The idea is to switch to Lmn index when voltage angle difference, δ is greater than 1.422 degrees and then switch to FVSI when it is less than 1.422 degrees as shown in table 4.2.

4.2.1.2 Simulation Result for the Base Case

Table 4.3 shows the base case values of the line stability indices and Figure 4.2 shows the bar charts of Lmn, FVSI and NLSI_1 against line Number. i.e. the twenty (20) interconnected lines of the IEEE 14-bus test system.

Table 4.3: The base case result for the IEEE 14-bus test system

Line No.	From Bus	To Bus	Voltage Stability Indices		
			Lmn	**FVSI**	**NLSI_1**
1	1	2	0.02795	0.02575	0.02795
2	1	5	0.08971	0.08029	0.08971
3	2	3	0.01043	0.00957	0.01043
4	2	4	0.01739	0.01626	0.01739
5	2	5	0.02699	0.02583	0.02699
6	3	4	0.1024	0.10618	0.10618
7	4	5	0.01086	0.01104	0.01104
8	4	7	0.0773	0.07702	0.0773
9	4	9	0.16108	0.15969	0.16108
10	5	6	0.09208	0.09094	0.09208
11	6	11	0.05762	0.05711	0.05711
12	6	12	0.0368	0.03618	0.03618
13	6	13	0.05731	0.05623	0.05623
14	7	8	0.06882	0.06882	0.06882
15	7	9	0.07662	0.07654	0.07654
16	9	10	0.00885	0.00882	0.00882
17	9	14	0.03355	0.03275	0.03275
18	10	11	0.03628	0.03641	0.03641
19	12	13	0.01944	0.01939	0.01939
20	13	14	0.05856	0.05765	0.05765

At base case, the simulation was carried out to obtain the voltage stability indices: the Lmn, FVSI and NLSI_1 using equations 3.14, 3.34 and 3.38, respectively. The MATLAB code used for the indices is as shown in appendix C. From Table 4.3 and Figure 4.2, the system is stable as none of the indices of each line is near 1. It is observed that the three indices' values are almost equal. This validates the fact that the developed new index, NLSI_1 index can be used in place of the other two indices.

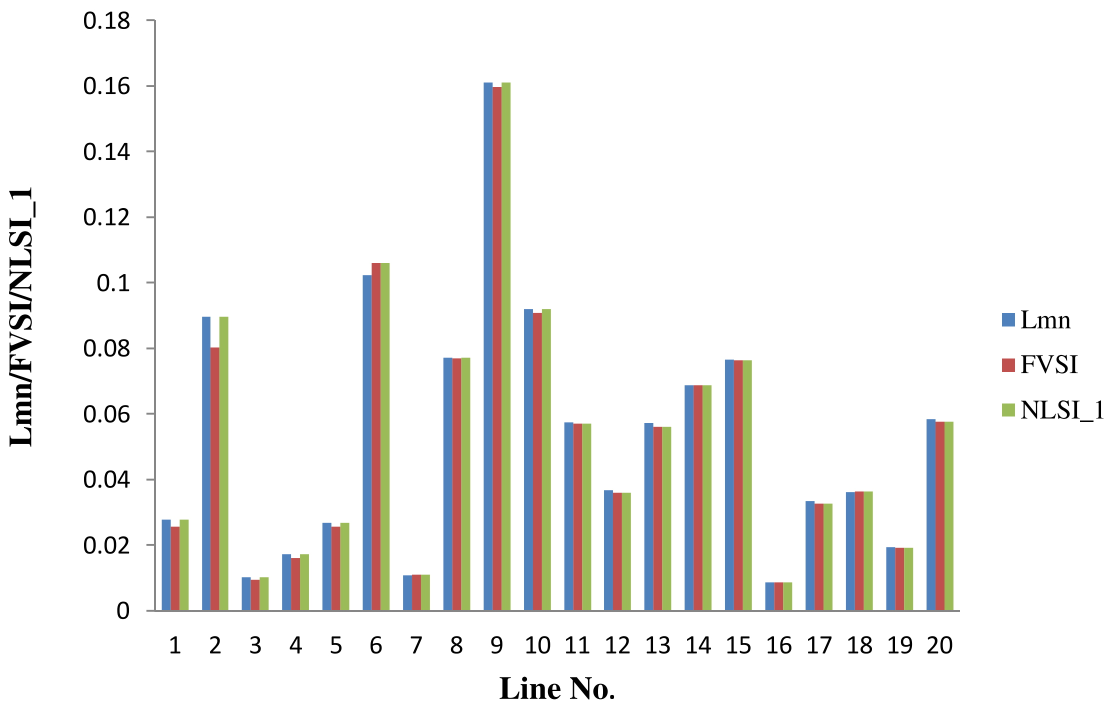

Figure 4.2: The bar chart of Lmn, FVSI and NLSI_1 Vs Line Number for the base case

4.2.1.3 Simulation Results for the Contingency Analysis

The contingency considered is the variation of the reactive power demand. This is carried out to determine the maximum loadability and critical line by varying the reactive load (Q MVAr) on the load buses until the value of the index approaches 1 or the power flow fails to converge. The reactive powers of the load buses were varied one at a time to investigate the maximum reactive power on all the load buses. This is done to determine the load-ability limit on each load bus, the ranking of the buses was carried out to identify the weak bus and critical lines with respect to a bus using the voltage stability indices that correspond to when the voltages become unstable. The weakest bus is hereby defined as the bus that has low load-ability limit and low voltage stability margin. This is the bus that requires compensation devices, or a PV solar generator, and / or voltage collapse relay for averting and mitigating against voltage collapse or instability.

The simulation result tabulated in Table 4.4 is for the determination of the maximum reactive load for all the load buses on the IEEE 14-bus system. Figure 4.3 shows the graph of the maximum reactive load (MVAr) against bus number. The maximum load-ability of each bus, the most critical line and most stable line with respect to a particular load bus are identified and tabulated as shown in Table 4.4. It is observed from Table 4.4, that the load buses with more interconnected lines accommodate higher reactive loads, which means that they are the most stable and reliable in the system, hence radial network is not desirable in power system networks. These load buses are 4 and 5 with maximum reactive loads of 361 and 352.5 MVAr respectively.

Table 4.4: Maximum Load for the Load Buses

Bus 4						
From	**To**	**Lmn**	**FVSI**	**NLSI_1**	**Ranking**	**Max Load MVAr**
3	4	0.94735	1.0305	0.94735	1	**361.0**
2	4	0.9315	0.89684	0.9315	2	
4	7	0.47528	0.47172	0.47528	3	
4	5	0.44293	0.44546	0.44546	4	
4	9	0.38756	0.38126	0.38756	5	
Bus 5						
From	**To**	**Lmn**	**FVSI**	**NLSI_1**	**RANKING**	**Max Load MVAr**
1	5	1.09165	0.9988	1.09165	1	**352.5**
5	6	0.88052	0.8552	0.88052	2	
2	5	0.87723	0.86374	0.86374	3	
4	5	0.37737	0.39075	0.37737	4	
Bus 7						
From	**To**	**Lmn**	**FVSI**	**NLSI_1**	**RANKING**	**Max Load MVAr**
7	8	0.99384	0.99384	0.99384	1	**165.5**
4	7	0.71677	0.71345	0.71345	2	
7	9	0.19249	0.19216	0.19216	3	
Bus 9						
From	**To**	**Lmn**	**FVSI**	**NLSI_1**	**RANKING**	**Max Load MVAr**
4	9	1.00065	0.98994	1.00065	1	**152.5**
7	9	0.61345	0.61234	0.61234	2	
9	14	0.47643	0.44712	0.47643	3	
9	10	0.21812	0.21509	0.21509	4	

Bus 10						
From	**To**	**Lmn**	**FVSI**	**NLSI_1**	**RANKING**	**Max Load MVAr**
10	11	0.99797	0.95642	0.99797	1	**121.8**
9	10	0.58473	0.60377	0.58473	2	
Bus 11						
From	**To**	**Lmn**	**FVSI**	**NLSI_1**	**RANKING**	**Max Load MVAr**
6	11	0.92693	0.99054	0.92693	1	**103.8**
10	11	0.44815	0.46769	0.44815	2	
Bus 12						
From	**To**	**Lmn**	**FVSI**	**NLSI_1**	**RANKING**	**Max Load MVAr**
12	13	1.06607	0.87059	1.06607	1	**78.9**
6	12	0.76222	0.8132	0.76222	2	
Bus 13						
From	**To**	**Lmn**	**FVSI**	**NLSI_1**	**RANKING**	**Max Load MVAr**
6	13	0.92585	0.99587	0.92585	1	**151.8**
12	13	0.63395	0.743	0.63395	2	
13	14	0.54454	0.50627	0.54454	3	
Bus 14						
From	**To**	**Lmn**	**FVSI**	**NLSI_1**	**RANKING**	**Max Load MVAr**
13	14	0.92337	0.97407	0.92337	1	**74.6**
9	14	0.86232	0.90106	0.90106	2	

Table 4.5 shows the maximum load-ability i.e. the maximum reactive load capacity of each bus and the bus ranking based on the load. The load bus with the least maximum load capacity is labeled as the weakest bus and the line as the critical and most

vulnerable line. From the rankings in Table 4.5, bus 14 has the least maximum load capacity (the smallest load among other maximum loads) and it ranks first i.e. the weakest bus.

Table 4.5: Maximum Load-Ability and Ranking for IEEE 14-Bus System

Bus No	from Bus	To bus	Vmag (pu)	Qmax (MVAr)	Lmn	FVSI	NLSI_1	Ranking
14	13	14	0.674	74.6	0.95474	1.00942	1.00942	1
12	12	13	0.88	78.9	1.06607	0.87059	1.06607	2
11	6	11	0.744	103.8	0.92693	0.99054	0.92693	3
10	10	11	0.652	121.8	0.59816	0.58365	0.58365	4
13	6	13	0.746	151.8	0.92585	0.99587	0.92585	5
9	4	9	0.703	152.5	1.00065	0.98994	1.00065	6
7	7	8	0.95	165.5	0.99384	0.99384	0.99384	7
5	1	5	0.771	352.5	1.09165	0.9988	1.09165	8
4	3	4	0.755	361	0.94735	1.0305	0.94735	9

In Figure 4.3, load bus 14 is the weakest and most vulnerable bus since it has the lowest maximum permissible reactive load of 74.6 MVAr. This bus has two (2) lines connected to it as shown in Table 4.4. Therefore, the critical line with respect to load bus 14 is the line 13-14. This implies that any addition of reactive load will lead to voltage collapse on the system. Bus 4 has the highest maximum load-ability and permissible reactive load of about 361MVAr.

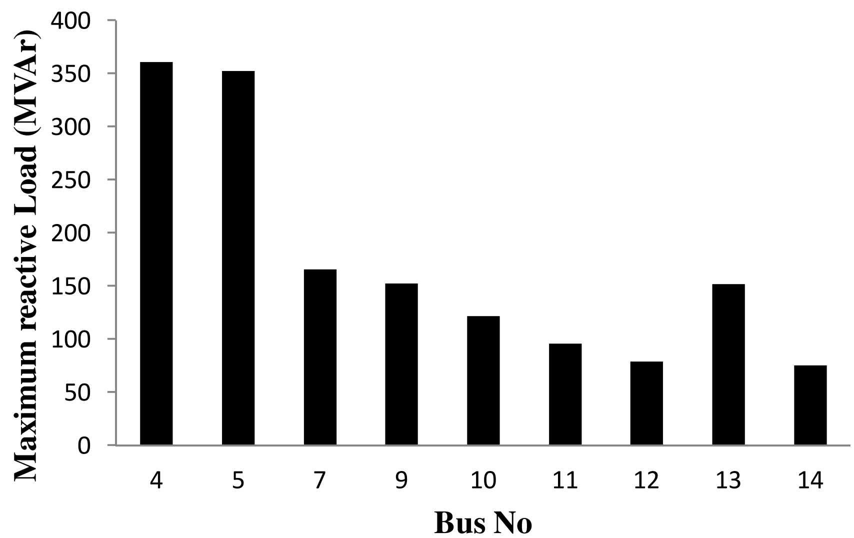

Figure 4.3: Maximum reactive load (Q MVAr) on load buses

The reactive power variation on bus 14 was carried out to investigate the indices with reactive load and the voltage characteristics. The results of this simulation are as presented in Table 4.6 while Figure 4.4 shows the graph of voltage magnitude and voltage stability indices (Lmn, FVSI and NLSI_1) against the reactive power Q (MVAr) variation for bus 14. It's worthy of note that the graphs of Lmn and NLSI_1 coincide, this gives credence to the new index, NLSI_1.

Table 4.6: Reactive power variations on bus 14

Q MVAr	Bus 14 -1st weakest bus (13-14)			
	Vmag pu	**Lmn**	**FVSI**	**NLSI_1**
5	0.946	0.05856	0.05765	0.05765
10	0.926	0.09758	0.09637	0.09637
20	0.887	0.17392	0.17287	0.17287
30	0.854	0.26946	0.26996	0.26996
40	0.822	0.39171	0.39623	0.39623
50	0.791	0.51545	0.52666	0.52666
60	0.752	0.66223	0.68451	0.66223
70	0.708	0.83048	0.86982	0.83048
75.6	0.674	0.95474	1.00942	0.95474

From Figure 4.4, for bus 14, it is observed that the curve of the voltage magnitude drops as the reactive power is increased while the voltage stability indices value also increase till voltage collapse occurs.

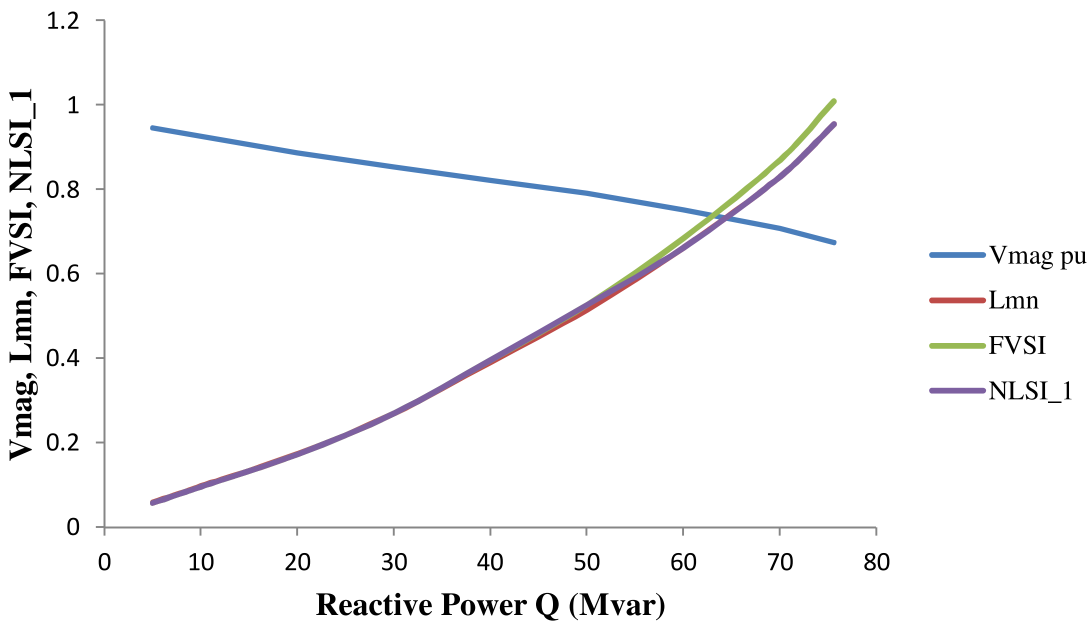

Figure 4.4: The graph of load variation on Bus 14

From Table 4.4, the maximum load-ability of each load bus, the most critical line and most stable line with respect to a particular load bus are identified and tabulated as shown in Table 4.7.

Table 4.7: IEEE 14-Bus System Load Bus Most Stable and Critical Line

S/No	Bus No	Max. Load (MVAr)	Most stable line	NLSI_1	Critical line	NLSI_1
1	4	361.0	4 – 9	0.38756	3 – 4	0.94735
2	5	352.5	4 – 5	0.37737	1 – 5	1.09165
3	7	165.5	7 – 9	0.19216	7 – 8	0.99384
4	9	152.5	9 – 10	0.21509	4 – 9	1.00065
5	10	121.8	9 – 10	0.58473	10 – 11	0.99797
6	11	103.8	10 – 11	0.44815	6 – 11	0.92693
7	12	78.6	6 – 12	0.76222	12 – 13	1.06607
8	13	151.8	14 -13	0.54454	6 – 13	0.92585
9	14	74.6	9 – 14	0.90106	13-14	0.92337

4.2.2 Simulation Results for the NNG 330-kV, 28-Bus Network

The power flow simulation for the NNG 330-kV, 28-bus network is herewith performed for the two scenarios: the base case and the contingency as mentioned earlier. The power flow study is used to calculate the voltage stability indices for the network (as shown in appendix B). The choice of Egbin power station bus as the slack bus for the load flow study is based on the fact that it has the generator with the largest power amongst the other power generating stations and the one with the lowest power mismatch in the network (Samuel *et al.*, 2014 (b)). The power flow solution is as shown in Table 4.8. Figure 4.5 shows the graph of the voltage profile of the NNG and Figure 4.6 shows the bar chart of voltage magnitude against buses that violated the voltage criteria (±5%) as set by NERC.

Table 4.8: Power Flow Solution Using Newton-Raphson Method for the NNG

Bus No	Bus Name	Voltage Mag. pu	Angle Degree	LOAD		GENERATOR		Injected MVAr
				MW	MVAr	MW	MVAr	
1	Egbin	1.05	0	0	0	182.638	589.599	0
2	Delta	1.05	15.424	0	0	670	82.628	0
3	Aja	1.04	-0.57	274.4	205.8	0	0	0
4	Akangba	0.97	0.482	344.7	258.5	0	0	0
5	Ikeja West	0.986	1.408	633.2	474.9	0	0	0
6	Ajaokuta	1.026	8.739	13.8	10.3	0	0	0
7	Aladja	1.046	14.04	96.5	72.4	0	0	0
8	Benin	1.011	9.306	383.4	287.5	0	0	0
9	Ayede	0.932	2.335	275.8	206.8	0	0	0
10	Osogbo	0.966	8.642	201.2	150.9	0	0	0
11	Afam	1.05	13.273	52.5	39.4	431	590.551	0
12	Alaoji	1.007	12.057	427	320.2	0	0	0
13	New Haven	0.905	3.322	177.9	133.4	0	0	0
14	Onitsha	0.949	6.268	184.6	138.4	0	0	0
15	Birnin-Kebbi	1.01	26.299	114.5	85.9	0	0	0
16	Gombe	0.844	4.905	130.6	97.9	0	0	0
17	Jebba	1.046	25.523	11	8.2	0	0	0
18	Jebba-GS	1.05	26.022	0	0	495	159.231	0
19	Jos	0.93	12.901	70.3	52.7	0	0	0
20	Kaduna	0.951	8.791	193	144.7	0	0	0
21	Kainji	1.05	31.819	7.5	5.2	624.7	-65.319	0
22	Kano	0.818	-1.562	220.6	142.9	0	0	0
23	Shiroro	1.05	13.479	70.3	36.1	388.9	508.034	0
24	Sapele	1.05	12.015	20.6	15.4	190.3	283.405	0
25	Calabar	0.951	21.703	110	89	0	0	0
26	Katampe	1	9.242	290.1	145	0	0	0
27	Okpai	1.05	46.869	0	0	750	193.093	0
28	AES-GS	1.05	5.871	0	0	750	488.128	0

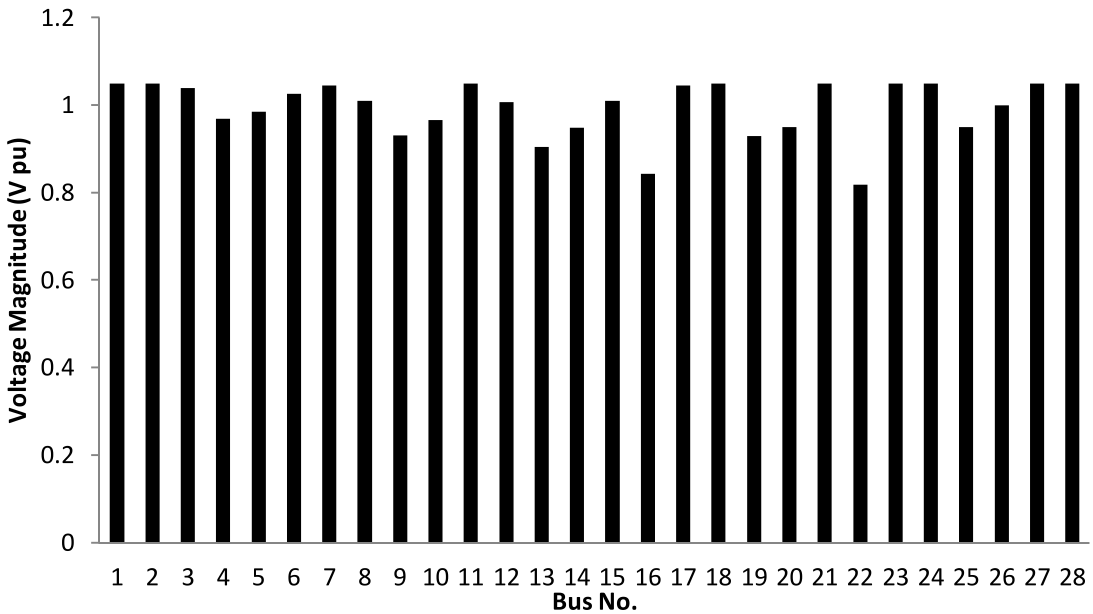

Figure 4.5:The Bar Chart of Voltage Magnitude Versus Bus Number for NNG 28-Buses.

The buses that violated the permissible voltage levels as set by NERC are as shown in Figure 4.6. In Figure 4.6, it is observed that the voltage profiles of buses 9, 13,14,16,19 and 22 (these are Kano, Gombe, New Haven, Jos, Ayede and Onitsha respectively) have the voltage magnitudes of 0.932, 0.905, 0.949, 0.844. 0.93 and 0.818 p.u respectively. These buses are considered to have violated the ±5% tolerance margin of voltage criterion. This low voltage is an indication that the network is prone or susceptible to possible voltage instability.

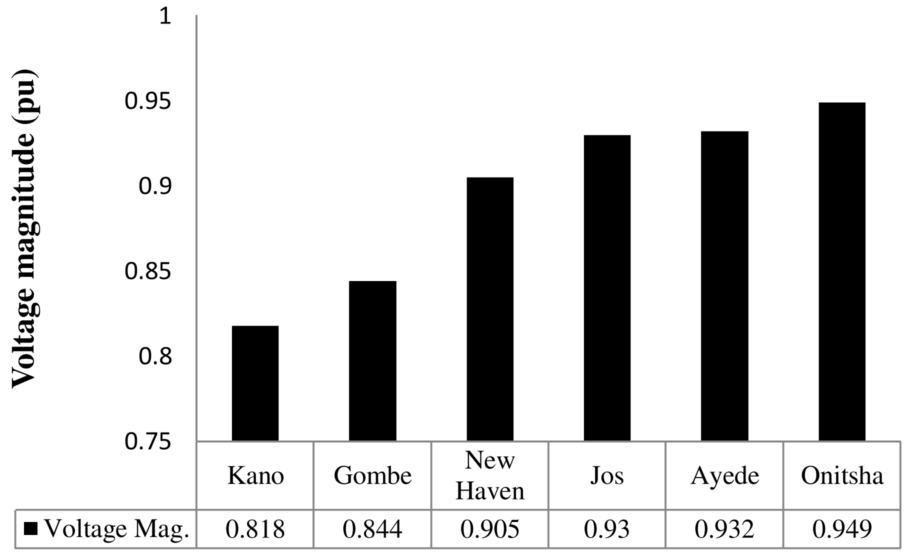

Figure 4.6: The Bar Chart of Voltage Magnitudes Versus Buses that Violated the Voltage Criteria

4.2.2.1 Determination of the Switching Function for 28-bus NNG System

Determination of the voltage angle difference for the switching function was carried out for the NNG 28-bus system as mentioned in section 4.2.2. The power flow solution results as shown in Table 4.8 are used for the base case simulation trial test for the two indices, Lmn and FVSI. Table 4.9 shows the data that helps determine the switching point based on the error percentage. The logic is to switch to Lmn index when voltage angle difference, δ is greater than 4.076 degrees and then switch to FVSI when it is less than 4.076 degrees as indicated in Table 4.9. At base case, the simulation was carried out to obtain the voltage stability indices: the Lmn, FVSI and NLSI_1 using equations 3.14, 3.34 and 3.38, respectively using the MATLAB code as shown in appendix C.

Table 4.9: Determination of the switching point for NNG 28-bus system

Line No	From bus	To bus	Lmn	Fvsi	Error %	$\delta = \delta_1 - \delta_2$
25	20	22	0.44501	0.41007	7.85151	10.351
30	25	27	0.17258	0.15969	7.469	-25.166
8	2	8	0.09927	0.09531	3.98912	6.114
18	12	14	0.15479	0.14911	3.66949	5.812
27	23	26	0.14388	0.14027	2.50904	4.236
24	19	20	0.22487	0.21952	2.37915	4.076
29	19	25	0.01242	0.01264	1.77134	-8.778
4	5	8	0.17865	0.1818	1.76322	-7.981
20	16	19	0.48726	0.49585	1.76292	-7.994
6	5	10	0.05505	0.05602	1.76204	-7.402
23	17	21	0.05023	0.0511	1.73203	-6.296
14	9	10	0.14574	0.14823	1.70852	-6.381
11	8	14	0.18005	0.17702	1.68287	3.031
28	12	25	0.2753	0.27984	1.64911	-9.675
15	15	21	0.30913	0.31421	1.64332	-5.52
26	20	23	0.36707	0.37267	1.5256	-4.702
31	5	28	0.22232	0.22567	1.50684	-4.45
19	13	14	0.17884	0.18081	1.10154	-2.952
10	7	24	0.04243	0.04197	1.08414	2.026
13	8	24	0.13579	0.13722	1.0531	-2.703
16	10	17	0.07707	0.07631	0.98612	-16.969
9	2	7	0.00203	0.00201	0.98522	1.385
17	11	12	0.15216	0.15122	0.61777	1.215
3	1	5	0.26412	0.26567	0.58685	-1.413
5	5	9	0.26094	0.2621	0.44455	-1.021
2	4	5	0.05629	0.05653	0.42636	-0.933
12	8	10	0.05957	0.05941	0.26859	0.579
7	6	8	0.02294	0.023	0.26155	-0.568
1	3	1	0.03404	0.03412	0.23502	-0.57
21	17	18	0.01305	0.01308	0.22989	-0.498

*Yellow shows the switching point.

4.2.2.2 Simulation Result for the Base Case

Table 4.10 shows the base case values of the line stability indices and Figure 4.7 shows the graph of Lmn, FVSI and NLSI_1 against line Number of the 31 interconnected lines of the NNG 330-kV, 28-bus network.

Table 4.10: The base case result for the NNG 330-kV, 28-bus network

L/No.	From Bus	To Bus	Lmn	FVSI	NLSI_1
1	3	1	0.03404	0.03412	0.03412
2	4	5	0.05581	0.05605	0.05605
3	1	5	0.24885	0.2503	0.2503
4	5	8	0.1699	0.17289	0.1699
5	5	9	0.18247	0.18321	0.18321
6	5	10	0.0271	0.02758	0.0271
7	6	8	0.02288	0.02293	0.02293
8	2	8	0.09332	0.08959	0.09332
9	2	7	0.00203	0.00202	0.00202
10	7	24	0.04242	0.04196	0.04196
11	8	14	0.18173	0.17866	0.17866
12	8	10	0.02329	0.02321	0.02321
13	8	24	0.12969	0.13106	0.13106
14	9	10	0.08997	0.0915	0.08997
15	15	21	0.30913	0.31421	0.31421
16	10	17	0.03779	0.03743	0.03779
17	11	12	0.15161	0.15068	0.15068
18	12	14	0.15131	0.1458	0.1458
19	13	14	0.17843	0.18039	0.18039
20	16	19	0.48733	0.49593	0.48733
21	17	18	0.01154	0.01155	0.01155
22	17	23	0.19823	0.17898	0.19823
23	17	21	0.05169	0.05259	0.05169
24	19	20	0.22523	0.21981	0.21981
25	20	22	0.44505	0.41011	0.44505
26	20	23	0.36738	0.37298	0.37298
27	23	26	0.14388	0.14027	0.14027
28	12	25	0.27511	0.27965	0.27511
29	19	25	0.01226	0.01247	0.01226
30	25	27	0.17269	0.15979	0.17269
31	5	28	0.20508	0.20818	0.20818

Table 4.10 and Figure 4.7 reveal that the system is stable as none of the line stability indices of each line is near to one (1). All the thirty one lines are in the range of stability index which is less than one (<1). It is observed that the three indices' values are almost equal. This phenomenon validates the fact that the newly developed index, NLSI_1 index can be used in place of the other two indices.

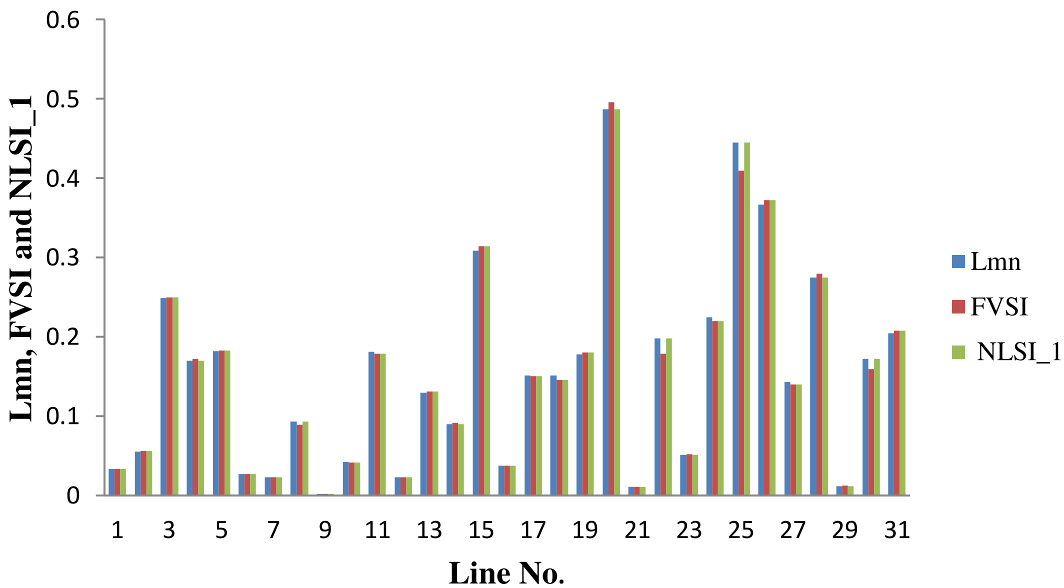

Figure 4.7: The bar chart of Lmn, FVSI and NLSI_1 Vs line number for the base case of the NNG 330-kV, 28-bus

4.2.2.3 Simulation results for the Contingency Analysis

The contingency analysis was carried out as explained in section 4.2.1.3. The simulation result is as presented in Table 4.11 for the determination of the maximum reactive load for all the load buses on the NNG 330-kV, 28-bus network. The reactive loads on the load buses were varied one at a time in an effort to identify the weak bus and critical line with respect to the bus. The values of maximum load are as presented in Table 4.11.

Table 4.11: Maximum reactive loads at the load buses of NNG network

Values of maximum reactive load of load buses of NNG							
Bus 3 – Aja							
From	To	Vmag	Lmn	FVSI	NLSI_1	Ranking	Max Load (MVAr)
3	1	0.842	1.00306	0.9993	0.9993		**3,948.5**
Bus 4 – Akangba							
From	To	Vmag	Lmn	FVSI	NLSI_1	RANKING	Max Load
4	5	0.62	0.99616	0.99846	0.99846		**1,881.9**
Bus 5- Ikeja							
From	To	Vmag	Lmn	FVSI	NLSI_1	RANKING	Max Load MVAr
5	28	0.79	0.98502	0.99987	0.99987	1	**2,438.9**
1	5		0.99123	0.99971	0.99971	2	
5	8		0.97755	0.99441	0.97755	3	
5	10		0.35327	0.35941	0.35327	4	
4	5		0.08837	0.08894	0.08894	5	
5	9		0.05755	0.05771	0.05771	6	
Bus 6 –Ajaokuta							
From	To	Vmag	Lmn	FVSI	NLSI_1	RANKING	Max Load MVAr
6	8	0.803	1.00101	0.997	0.997		**273.8**
Bus 7-Alaidja							
From	To	Vmag	Lmn	FVSI	NLSI_1	RANKING	Max Load MVAr
24	7	0.808	1.01375	0.99198	0.99198	1	**2,565.9**
2	7		0.76468	0.7639	0.7639	2	
Bus 8- Binin							
From	To	Vmag	Lmn	FVSI	NLSI_1	RANKING	Max Load MVAr
8	24	0.796	0.99059	0.9992	0.9992	1	**2,073.9**
2	8		0.946	0.91323	0.91323	2	
8	10		0.68872	0.68406	0.68406	3	
5	8		0.59238	0.60251	0.59238	4	
8	14		0.13399	0.12945	0.12945	5	
6	8		0.0371	0.03723	0.03723	6	

Bus 9- Ayede							
From	To	Vmag	Lmn	FVSI	NLSI_1	RANKING	Max Load MVAr
9	10	0.658	0.9939	1.0113	0.9939	1	**778.8**
Bus 10 – Osogbo							
From	To	Vmag	Lmn	FVSI	NLSI_1	RANKING	Max Load
10	17	0.762	0.99847	0.97592	0.99847	1	**832.5**
8	10		0.76053	0.76355	0.76355	2	
5	10		0.74076	0.75253	0.74076	3	
9	10		0.15632	0.15895	0.15632	4	
Bus 12- Olaoji							
From	To	Vmag	Lmn	FVSI	NLSI_1	RANKING	Max Load MVAr
11	12	0.752	0.98961	0.99132	0.99132	1	**2,572.5**
12	14		0.30864	0.29726	0.29726	2	
12	25		0.00613	0.00614	0.00613	3	
Bus 13 - New Haven							
From	To	Vmag	Lmn	FVSI	NLSI_1	RANKING	Max Load MVAr
13	14	0.654	0.9824	0.99516	0.99516	1	**384.5**
Bus 14- Onitsha							
From	To	Vmag	Lmn	FVSI	NLSI_1	RANKING	Max Load MVAr
8	14	0.711	1.01712	0.99653	0.99653	1	**656.3**
12	14		0.98924	0.95081	0.98924	2	
13	14		0.34982	0.3555	0.3555	3	
Bus 15 -B-kebbi							
From	To	Vmag	Lmn	FVSI	NLSI_1	RANKING	Max Load MVAr
15	21	0.866	0.97797	0.99391	0.99391		**199.9**
Bus 16 – Gombe							
From	To	Vmag	Lmn	FVSI	NLSI_1	RANKING	Max Load MVAr
16	19	0.71	0.98194	0.99824	0.98194	1	**139.5**

Bus 17 – Jebba							
From	To	Vmag	Lmn	FVSI	NLSI_1	RANKING	Max Load MVAr
17	23	0.889	0.99986	0.86017	0.99986	1`	**5,639.2**
17	21		0.63544	0.64635	0.63544	2	
17	18		0.49989	0.49976	0.49976	3	
10	17		0.35371	0.3437	0.35371	4	
Bus 19 – Jos							
From	To	Vmag	Lmn	FVSI	NLSI_1	RANKING	Max Load MVAr
19	16	0.756	0.99999	1.00582	0.99999	1	**232.5**
19	20		0.83364	0.80442	0.80442	2	
19	25		0.46203	0.46884	0.46203	3	
Bus 20 – Kaduna							
From	To	Vmag	Lmn	FVSI	NLSI_1	RANKING	Max Load MVAr
20	23	0.832	0.9813	0.9963	0.9963	1	**418.9**
20	22		0.91981	0.79724	0.91981	2	
19	20		0.09629	0.09345	0.09345	3	
Bus 22 – Kano							
From	To	Vmag	Lmn	FVSI	NLSI_1	RANKING	Max Load MVAr
20	22	0.674	0.99681	0.89417	0.99681		**202.6**
Bus 25 – Calabar							
From	To	Vmag	Lmn	FVSI	NLSI_1	RANKING	Max Load MVAr
12	25	0.761	0.9927	1.00057	0.9927	1	**462.7**
25	27		0.59301	0.51796	0.59301	2	
19	25		0.09268	0.09345	0.09268	3	
Bus 26 – Katampe							
From	To	Vmag	Lmn	FVSI	NLSI_1	RANKING	Max Load MVAr
23	26	0.745	1.00227	0.97507	0.97507	1	**632**

It is observed from Table 4.11 that the load buses with more interconnected lines accommodate higher reactive loads. This means that they are the most stable and reliable in the system, hence radial lines are not desirable in power system networks.

This is in agreement with the mostly reported radial nature of the NNG system which makes it to experience voltage collapse more often. The load buses that accommodate high reactive power are buses 3, 5, 8, 12 and 17 with maximum reactive loads of 3,948.5, 2,438.9, 2,073.9, 2,572.5 and 5,639.2 MVAr, respectively.

From Table 4.11, the maximum load-ability of each load bus, its critical line and the most stable line with respect to a particular load bus are identified and tabulated in Table 4.12. Table 4.12 present the rankings of all the load buses on the NNG system with bus 16 (Gombe) ranking first as the weakest while bus 17 (Jebba) ranks as the nineteenth (19^{th}) bus as the best i.e. most stable, reliable and strongest.

Table 4.12: Maximum load-ability and the ranking of load buses on NNG

From Bus	**To Bus**	**Bus Name**	**Bus No**	**Qmax. (MVAr)**	**Voltage mag (pu)**	**Voltage stability indices**			
						Lmn	**FVSI**	**NLSI_1**	**Ranking**
16	**19**	**Gombe**	**16**	**139.5**	**0.71**	**0.98194**	**0.99824**	**0.98194**	**1**
15	21	B-kebbi	15	199.9	0.866	0.97797	0.99391	0.99391	2
20	22	Kano	22	202.6	0.674	0.99681	0.89417	0.99681	3
16	19	Jos	19	232.5	0.756	0.99999	1.00582	0.99999	4
6	8	Ajaokuta	6	273.8	0.803	1.00101	0.997	0.997	5
13	14	N/ haven	13	384.5	0.654	0.9824	0.99516	0.99516	6
20	23	Kaduna	20	418.9	0.832	0.9813	0.9963	0.9963	7
12	25	Calabar	25	462.7	0.761	0.9927	1.00057	0.9927	8
23	26	Katampe	26	632	0.745	1.00227	0.97507	0.97507	9
8	14	Onitsha	14	656.3	0.711	1.01712	0.99653	0.99653	10
9	10	Ayede	9	778.8	0.658	0.9939	1.0113	0.9939	11
10	17	Oshogbo	10	832.5	0.762	0.99847	0.97592	0.99847	12
4	5	Akangba	4	1881.9	0.62	0.99616	0.99846	0.99846	13
8	24	Benin	8	2073.9	0.796	0.99059	0.9992	0.9992	14
5	28	Ikeja	5	2438.9	0.79	0.98502	0.99987	0.99987	15
24	7	Aladja	7	2565.9	0.808	1.01375	0.99198	0.99198	16
11	12	Alaoji	12	2572.5	0.752	0.98961	0.99132	0.99132	17
3	1	Aja	3	3948.5	0.842	1.00306	0.9993	0.9993	18
17	23	Jebba	17	5639.2	0.889	0.99986	0.86017	0.99986	19

Figure 4.8 shows the graph of maximum reactive load (MVAr) against bus number. It is observed that load bus 16 is the weakest and most vulnerable bus since it has the lowest maximum permissible reactive load of 139.5 MVAr. This bus has one (1) line connected to it. Therefore, the critical line with respect to load bus 16 is the line 16-19. This implies that any additional reactive load will lead to voltage collapse on the system.

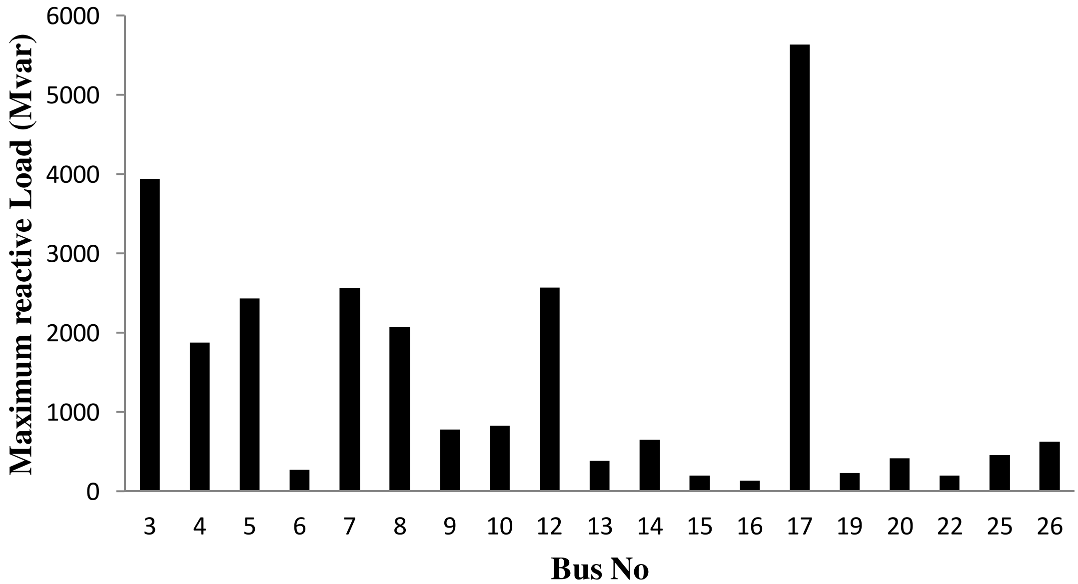

Figure 4.8: Maximum reactive loads (Q MVAr) at load buses of NNG

The reactive power variations were carried out on bus 16, (Gombe) showing the impact of voltage magnitude (pu) and the Lmn, FVSI and NLSI_1 on the most critical line (16-19). The result is as presented in Table 4.13. Figure 4.9 shows the graphs of Vmag, Lmn, FVSI and NLSI_1 against the reactive load variation on bus 16.

Table 4.13: Reactive power variations on load bus 16 (Gombe)

S/No.	Q (MVAr	Vmag (pu)	Lmn	FVSI	NLSI_1
1	0	1.028	0	0	0
2	15	1.005	0.05272	0.05364	0.05272
3	30	0.98	0.11077	0.11273	0.11077
4	45	0.954	0.17535	0.17845	0.17535
5	60	0.926	0.24807	0.25246	0.24807
6	75	0.896	0.33128	0.33714	0.33128
7	90	0.863	0.42857	0.43614	0.42857
8	105	0.826	0.54588	0.55549	0.54588
9	120	0.783	0.69438	0.70646	0.69438
10	135	0.73	0.9	0.91519	0.9
11	139.5	0.71	0.98229	0.99859	0.98229

From Figure 4.9 for the weakest bus 16, it is observed that the curve of the voltage magnitude drops as the reactive power is increased while the voltage stability indices' values also increase till voltage collapse occurs. The NLSI_1, as can be seen, gives the true representation of Lmn and the FVSI indices hence the NLSI_1 could be used instead of using the Lmn and FVSI individually and improving the voltage stability assessment of PSNs.

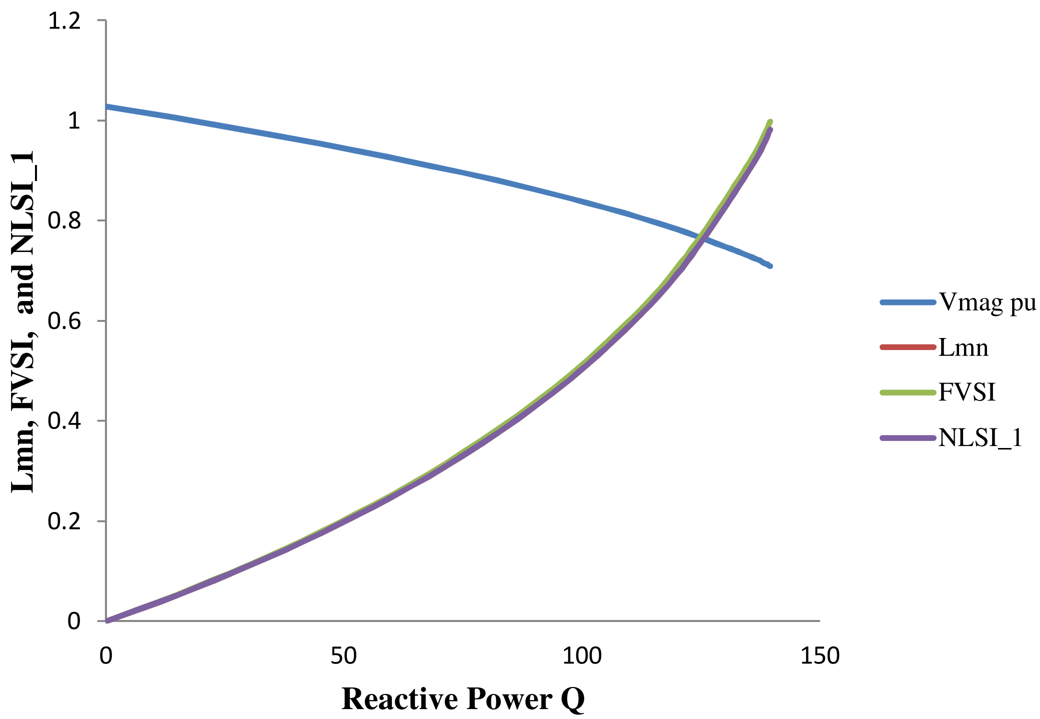

Figure 4.9: The graphs of load variations on Bus 16

It is observed from figure 4.9, that the graph of Lmn almost coincides with that of NLSI_1 thus making them appear as one graph hence showing that the new index, NLSI_1 compares, to a very large extent, with the other indices.

From Table 4.11, the maximum load-ability of each load bus, the most critical line and most stable line with respect to a particular load bus are identified and tabulated as shown in Table 4.14.

Table 4.14: The NNG 28-Bus System Load Bus Most Stable and Critical Line

S/No	Bus No	Bus Name	Max. Load (MVAr)	Most stable lines	NLSI_1	Critical lines	NLSI_1
1	3	Aja	3948.5	Nil	Nil	3 – 1	0.99930
2	4	Akangba	1881.9	Nil	Nil	4 – 5	0.99846
3	5	Ikeja	2438.9	5 – 9	0.05771	2 – 28	0.99987
4	6	Ajaokuta	273.8	Nil	Nil	6 – 8	0.99700
5	7	Alaidja	2565.9	2 – 7	0.7639	24 – 7	0.99198
6	8	Benin	2073.9	8 – 24	0.03723	6 – 8	0.99920
7	9	Ayede	778.8	Nil	Nil	24 – 7	0.99390
8	10	Osogbo	832.5	9 -10	0.15632	17- 10	0.99847
9	12	Olaoji	2572.5	12 – 25	0.00613	11 – 12	0.99132
10	13	NewHaven	384.5	Nil	Nil	13- 14	0.99516
11	14	Onitsha	656.3	13-14	0.3555	8 – 14	0.99653
12	15	B- Kebbi	199.9	Nil	Nil	15 – 21	0.99391
13	16	Gombe	139.5	Nil	Nil	16 – 19	0.98194
14	17	Jebba	5639.2	10 – 17	0.35371	17 – 23	0.99986
15	19	Jos	232.5	19 – 25	0.46203	19 – 16	0.99999
16	21	Kaduna	418.9	19 – 20	0.09345	20 – 23	0.99630
17	22	Kano	202.6	Nil	Nil	20 – 22	0.99681
18	25	Calaba	462.7	25 – 19	0.09268	12 – 25	0.99270
19	26	Katenpe	632	Nil	Nil	23 – 26	0.97507

4.3 Discussion of the Results

The newly developed voltage stability index, NLSI_1, has a switching logic that depends on the voltage angle difference since FVSI fails when the angle difference is large. Therefore, it has the advantage of fastness and its accuracy when voltage angle difference is small. Large voltage angle different is a precursor to voltage collapse (Dobson *et al.,*2010). The Lmn has the advantage of being accurate since the phasor part is included in its expression, so the newly developed index uses these advantages for improved voltage stability indice. The new line stability index-1 (NLSI_1) developed in the research was simulated and compared with the Lmn and FVSI indices on the IEEE 14-bus test system for its validation and subsequently, on the NNG 28-bus practical system to enable these indices to be evaluated **for the first time**. The results are hereby discussed.

4.3.1 Discussion of the simulation results for the IEEE 14-bus test system

The simulation results for the IEEE 14-bus test system, for the base case, show that the system is stable because the three indices' values are approximately equal and they are less than one (<1). For the contingency case, bus 14 was revealed to be the weakest bus as the indices' values are very close to one (~1). This implies proximity to voltage collapse and it has the smallest maximum permissible reactive loading of 74.6MVAr. This means that bus 14 is the optimal location for the placement of a possible compensating device for improving the voltage profile at the bus as a measure against voltage collapse (Reis *et al.*, 2009; Telang and Khampariya, 2015; Tilwani and Choube, 2015). A comparative assessment of some voltage collapse indices (PV curve, QV curve, modal analysis, L-Index) was carried out on the IEEE 14-bus testing system. They gave virtually the same results as the newly developed NLSI_1 of this thesis. The simulations indicate that the bus 14 of IEEE 14-bus system is the weakest in the system as NLSI_1 also revealed. The voltage at which the bus is on maximum permissible load is referred to as the **critical voltage** for bus 14 is 0.674 p.u.

Subramani *et al.*, (2012) using the line stability index, Lmn, also gave bus 14 as the weakest bus with permissible load of 73MVar and Line 13-14 as the critical line while the newly developed index of this thesis i.e. NLSI_1 has 74.6 MVAr as its maximum permissible reactive load and the Line 13 - 14 as the critical line of the system. As can be seen, the results are relatively comparable.

Sinha and Chauhan, (2014). Uses the FVSI, and have bus 14 as its weakest bus with maximum permissible load of 74 MAVr as against 74.6 MAVr for the NLSI_1 which is also very close. The critical line is also line 13-14. These results show that the new line index developed is valid and accurate since the results compares favourably well with those obtained for the IEEE 14-bus test system in the technical literatures.

4.3.2 Discussion of the Simulation Results for the NNG 28-Bus test System

The new line stability index of this thesis was also applied to the current 28-bus, 330-kV Nigerian National Grid. Bus 16 (Gombe) was found to be the weakest load bus in the system with the maximum permissible reactive power load of 139.5 MVAr and the **critical voltage** is 0.71 p.u. This means that any increase in the reactive power load beyond the quoted figure will probably lead to voltage collapse. Bus 16 is then the optimal location for a possible compensating device. The weakest line here is the line 16-19. This newly developed line stability index-1 (NLSI_1) in this work is accurate and fairly comparable with the other indices. It can be used as a single voltage stability index instead of using the Lmn and FVSI separately because it combines the accuracy of Lmn and the fastness of FVSI.

Conventionally, voltage magnitude is used as an indication of a possible voltage instability but that is not generally true as an indication of proximity to voltage collapse and location for optimal placement of compensating device as revealed by the voltage profile of the buses that violated the 0.95 p.u criterion (Abdulkareem *et al.*, 2016). Foe example, Kano has the least voltage magnitude with 0.818 p.u as against Gombe with voltage magnitude of 0.844 p.u. If the criterion is based on voltage magnitude, Kano will be erroneously picked as the weakest bus but the use of the of the index criterion, Gombe with a higher voltage magnitude is the actual weakest bus because of its superior index value.

The most stable lines are lines with the least voltage stability indices while the critical lines are the lines with the highest values of the voltage stability indices with respect to individual load buses. It can be seen that the line connected to individual load bus with the lowest stability index value is the most stable line while the line with the highest stability index value is the critical lines with respect to that particular load bus as shown in Tables 4.7. and 4.14.

4.4 Summary

Simulations were carried out based on two scenarios. The two scenarios are the base case and the contingency in this chapter. The results and discussions were presented. It can be said that the NLSI_1 can be used in its present form instead of using the other two indices for the prediction of voltage collapse and identification of both the weakest bus and critical lines in a system for the reasons advanced earlier on.

CHAPTER FIVE

CONCLUSIONS AND RECOMMENDATIONS

5.1 Summary

In this research work, a new line stability index-1 (NLSI_1) has been developed for the prediction of voltage collapse in power system networks. It is a powerful tool for identifying the weakest bus in the network, the critical and most vulnerable line with respect to a particular load bus. This will eventually help to locate the area for load shedding and also for determining the maximum load-ability of the load buses. This will consequently guide the operator to take quick action to avert the voltage collapse when a particular bus is being overloaded and where to place compensation devices will be so revealed.

5.2 Achievements and Contribution to Knowledge

The main contributions of this study are summarized as follows:

1) A new line voltage stability index suitable for the prediction of voltage collapse of power system networks was developed in this research and this contribute to the present body of knowledge in voltage stability studies.

2) An associated software programme (based on this new index) for simulation and implementation of voltage stability indices was successfully developed and implemented in the MATLAB environment. This will provide a toolkit for researchers in the study domain.

3) The results of this research engender accurate identification of critical lines and weak areas, vulnerable or weak load bus on the 28-bus, 330kV, NNG for optimum placement of compensating devices and load shedding relays on the network to avert voltage collapse.

4) The development of the new stability index in its present form can be applied to any power system for stability analysis and voltage collapse prediction in Nigeria and other parts of the world.

5.3 Recommendations for Future Work

a) Incorporating modeling and analysis of compensating devices such as generators and compensating devices using the developed novel line stability index to improve voltage stability of power system networks can be a good extension of the work reported in this thesis.

b) For ease of gathering data for future work of this nature, it is recommended that operators of the transmission networks in Nigeria, TCN, should install phasor measurement units (PMUs) on the national grid in order to facilitate real time analysis and accurate data gathering.

REFERENCES

Abdulkareem, A., Awosope, C. O. A., Samuel, I. A., & Agbetuyi, A. F. (2016). Contingency Analysis for Assessing Line Losses in Nigeria 330-kV Power lines. *International Journal of Engineering and Advanced Technology*, *5*(3), 66-78.

Adebayo, A. G., Jimoh, A., Yusuff, A., & Adeyemi, (2014). A. Effects Of Phase Shifting Transformers on Weak and Ill-Conditioned Network: Nigerian 330kV Grid System. *power*, *13*, *International Conference of power and Energy Systems (Africa PSE 2014)*. Gaboroune, Botswana. p. 14.

Afolabi, O. A., Ali, W. H., Cofie, P., Fuller, J., Obiomon, P., & Kolawole, E. S. (2015). Analysis of the Load Flow Problem in Power System Planning Studies. *Energy and Power Engineering*, *7*(10), 509.-523.

Ajjarapu, V., & Meliopoulos, A. S. (2008). Preventing voltage collapse with protection systems that incorporate optimal reactive power control. *PSERC Publication*, 08-20.

Ali, N. A. (2005). An Overview of system collapses on the Nigerian Grid Network. In *Proceedings of the International Conference on Power Systems Operations and Plaing-VI (ICPSOP)* (pp. 67-70).

Amoda, O. (2007). Deregulation in Nigeria: History Overview, Motivation, Status and Recommendation. *The Nigerian village Square*.

Andersson, G., Donalek, P., Farmer, R., Hatziargyriou, N., Kamwa, I., Kundur, P., ... & Schulz, R. (2005). Causes of the 2003 major grid blackouts in North America and Europe, and recommended means to improve system dynamic performance. *IEEE transactions on Power Systems*, *20*(4), 1922-1928.

Anyanwu, C. A. (2005). State of Power System Operation and Planning the Nigerian Power System. In *Proceedings of the International Conference on Power Systems Operations and Planning-VI (ICPSOP)* (pp. 103-108).

Arya, L. D., & Shrivastava, M. (2006). Voltage stability evaluation using line voltage stability index. *IE (I) Journal-El*, *87*.

Balamourougan, V., Sidhu, T. S. and Sachdev, M. S. (2004). Technique for online prediction of voltage collapse. *IEE Proceedings-Generation, Transmission and Distribution*, *151*(4), 453-460.

Bhaladhare, S., Telang, A. and Bedekar, P. (2013). PV, QV Curve–A Novel Approach for Voltage Stability Analysis. *International Journal of Computer Applications®(IJCA)*.

Telang B. and Khampariya P. (2015). Voltage Stability Evaluation Using Modal Analysis. *International Journal of Scientific Research Engineering & Technology (IJSRET), 4*(4), 408-411.

Channelstv. (2015). *Channels*. Retrieved June 08, 2016, from http://www.channelstv.com/: http://www.channelstv.com/2015/09/13/nigeria-loses-100-billion-to-daily-blackout/

Chawla, P., & Singh B., (2013) Voltage Stability Assessment and Enhancement Using STATCOM-A Case Study. World Academy of Science, Engineering and Technology. International Journal of Electrical, Computer, Energetic, Electronic and Communication Engineering Vol:7, No:12, pp1269-1274.

Chayapathi, V., Sharath, B., & Anitha, G. S.(2013) Voltage Collapse Mitigation By Reactive Power Compensation At The Load Side. International Journal of Research in Engineering and Technology. 2(9).

Dharamjit, & Tanti D. K. (2012). Load Flow Analysis on IEEE 30 bus System. *International Journal of Scientific and Research Publications*, *2*(11). pp 1-6.

Dobson, I., Parashar, M., & Carter, C. (2010). Combining phasor measurements to monitor cutset angles. In *System Sciences (HICSS), 2010 43rd Hawaii International Conference on* (pp. 1-9). IEEE.

Donna R. (2012). *Algebra lesson page*. Retrieved Febrary 12, 2016, from Error in Measurement: http://www.regentsprep.org/regents/math/algebra/am3/LError.htm

Enemuoh, F. O., Onuegbu, J. C., & Anazia, E. A. (2013). Modal based analysis and evaluation of voltage stability of bulk power system. *International Journal of Engineering Research and Development*, *6*(12), 71-79.

Fink, L. & Carlsen, K. (1978). Operating under stress and strain. *IEEE Spectrum;(United States)*, *15*(3).

Gao, B., Morison, G. K. & Kundur, P. (1992). Voltage stability evaluation using modal analysis. *IEEE Transactions on Power Systems*, *7*(4), 1529-1542.

Goh, H. H., Chua, Q. S., Lee, S. W., Kok, B. C., Goh, K. C. & Teo, K. T. K. (2014). Line voltage stability indices based on precautionary measure approximation in smart grid. *Proceedings of the 11th International Conference on Innovation & Management* (pp. 1507-1518). Finland, the University of Vaasa.

Goh, H. H., Chua, Q. S., Lee, S. W., Kok, B. C., Goh, K. C. & Teo, K. T. K. (2015). Comparative study of line voltage stability indices for voltage collapse forecasting in power transmission system. *Rio de Janeiro Brazil, 13*(2), 270-275.

Gunadin, I. C., Soeprijanto A. & Penangsang O. (2012). Steady State Stability Assessment Using Extreme Learning Machine Based on Modal Analysis. (Vol. 7). International Review of Electrical Engineering (I.R.E.E.), pp 1-6 http://repository.unhas.ac.id/bitstream/handle/123456789/7095/Indar_IREE%20 Journal_ID_8173.pdf?sequence=1

Haruna, M. (2015). An Overview on Voltage Stability Indices as Indicators of Voltage Stability for Networks with Distributed Generations Penetration. *International Journal of Science, Technology and Society*. (3)4, pp. 214-219.

Hasani, M. and Parniani, M. (2005). Method of combined static and dynamic analysis of voltage collapse in voltage stability assessment. In *2005 IEEE/PES Transmission & Distribution Conference & Exposition: Asia and Pacific* (pp. 1-6). IEEE.

Kessel, P., & Glavitsch, H. (1986). Estimating the voltage stability of a power system. *IEEE Transactions on Power Delivery*, *1*(3), 346-354.

Kodsi, S. M. and Canizares, C. A. (2003). Modeling and simulation of IEEE 14 bus system with facts controllers. *University of Waterloo, Canada, Tech. Rep*.

Kumarswamy, I., and Ramanareddy, P. (2011). Analysis of Voltage Stability Using L-Index Method. *international Journal of Electrical Engineering, 4*(4), 483-498.

Kundur, P. (1994). Power System Stability and Control, McGrew-Hill.

Kundur, P., Paserba, J., Ajjarapu, V., Andersson, G., Bose, A., Canizares, C., ... and Van Cutsem, T. (2004). Definition and classification of power system stability IEEE/CIGRE joint task force on stability terms and definitions. *IEEE transactions on Power Systems*, *19*(3), 1387-1401.

Lamine, M. (2011). *Taxonomy of the Characteristics of Power System Operating States* Northern Virginia Center, Virginia Tech, Bradley Department of Electrical and Computer Engineering. Virginia Tech: Retrieved May 12, 2016 www.nvc.vt.edu/lmili/.../RESIN_Workshop_2011-White_Paper-Mili.pdf.

Liacco, T. D. (1967). The adaptive reliability control system. *IEEE Transactions on Power Apparatus and Systems*, *5*(PAS-86), 517-531.

Mathew, M., Babu, D. S., Venkataramu, P. S., & Nagaraj, M. S. (2015). Effect of TCSC on Line Voltage Stability Indices under Single Line Outage Condition. International Journal Of Innovative Research in Electrical, Electronics, Instrumentation and Control Engineering, *3*(8), 101-105.

Moghavvemi, M., & Omar, F. M. (1998). Technique for contingency monitoring and voltage collapse prediction. *IEE Proceedings-Generation, Transmission and Distribution*, *145*(6), 634-640.

Mohamed, A., Jasmon, G. B., & Yusoff, S. (1989). A static voltage collapse indicator using line stability factors. *Journal of industrial technology*, *7*(1), 73-85.

Morison, G. K., Gao, B., & Kundur, P. (1993). Voltage stability analysis using static and dynamic approaches. *IEEE Transactions on Power Systems*, *8*(3), 1159-1171.

Musirin, I., & Rahman, T. A. (2002). Novel fast voltage stability index (FVSI) for voltage stability analysis in power transmission system. In *Research and Development, 2002. SCOReD 2002. Student Conference on* (pp. 265-268). IEEE.

Nayak, N., & Wadhwani, A. K. (2014). Performance of Newton-Raphson Techniques in Load Flow Analysis using MATLAB. *International Journal of Engineering and Technical Research ISSN: 2321-0869*, pp, 177-180.

Ndiagwalukwe, J. U. (2012, May, 2012 11th -12th). Strategies For Mitigating Incidence Of System Collapse. Retrieved August 14, 2015, from http://slideplayer.com/slide/3179976/

Nigeria Electricity Regulatory Commission, (2005). The Grid Code for the Nigeria Electricity Transmission System. Electrical power sector reform Act, version 01.2005.

Nizam, M., Mohamed, A., & Hussain, A. (2007). Voltage collapse prediction incorporating both static and dynamics analyses. *European Journal of Scientific Research*, *16*(1), 10-25.

Ogbonna, A. (2015). Nigeria loses $100b to daily power outage. *vanguard*, p. 1.

Onahaebe, O., & Apeh, S. (2007). Voltage Instability in Electrical Network: A case study of Nigerian 330kV Transmission Grid. *Research Journal of Applied Sciences*, *2*(8), 865-874.

Oleka, E. U., Ndubisi, S. N., & Ijemaru, G. K. (2016). Electric Power Transmission Enhancement: A Case of Nigerian Electric Power Grid. *American Journal of Electrical and Electronic Engineering*, *4*(1), 33-39.

Padiyar, K. (1996). *Power System Dynamics - Stability and Control.* Interline Publishing Pvt. Ltd.

Power Holding Company of Nigeria (2010) Generation and Transmission Grid Operations 2009. National Control Centre, Osogbo Annual Technical Report.

Pourbeik, P., Kundur, P. S., & Taylor, C. W. (2006). The anatomy of a power grid blackout. *IEEE Power and Energy Magazine*, *4*(5), 22-29.

Quintela, A. S., & Castro, C. A. (2002). Improved branch-based voltage stability proximity indices. II. Application in security analysis. In *Power Engineering 2002 Large Engineering Systems Conference on, LESCOPE 02*(pp. 115-119). IEEE.

Rajabi, A. R., Rashnoei, S., Hakimzadeh, M., & Habibi, A. (2014). Coordination between SC and SVC for Voltage Stability Improvement. *World Academy of Science, Engineering and Technology, International Journal of Electrical, Computer, Energetic, Electronic and Communication Engineering*, *8*(9), 1443-1446.

Reddy, R. S. S., & Manohar, T. G. (2012). Literature Review on Voltage stability phenomenon and Importance of FACTS Controllers In power system Environment. *GJRE-F: Electrical and Electronic Engineering*, *12*(3), 25-29

Saadat, H. (2004). *Power System Analysis* (Second ed.). Singapore: Mc Graw Hill.

Samuel, I. A., Katende, J., Daramola, S. A., & Awelewa, A. A. (2014), (a). Review of System Collapse Incidences on the 330-kV Nigerian National Grid. *International Journal of Engineering Science Invention*, *3*, 55-59

Samuel, I. A., Okwechime, N. M., & Abdulkareem, A. (2014), (b). Investigating The Selection Of A Suitable Slack Bus: A Case Study Of The Multi-Generating Stations Of The Nigerian 330-kV Power System Network. *International Journal of Electrical Electronic Engineering Studies*, *2*(1), 1-12.

Sanaye-Pasand, M., & Rezaei-Zare, A. (2003). Review and Simulation of Static Indices in Detection of Proximity to Voltage Collapse. In *Australian Universities Power Engineering Conference*.

Sarat K. S., Suresh S. R. & Jayaram Kumar S.V. (2012). New Voltage Stability Index (NVSI) for Voltage Stability Analysis in Power System. *International Journal of Electrical and Electronics Engineering Research (IJEEER), 2*(4), 13-20.

Sinha, R.K. and Chauhan, S.(2014) Fast Contingency Analysis and Ranking for Power System Security Assessment. Proceedings of Thirteenth IRF International Conference, Chennai, India, ISBN: 978-93-84209-51-3. Pp116-121.

Subramani, C., Dash, S. S., Kumar, V., & Kiran, H. (2012). Implementation of line stability index for contingency analysis and screening in power systems. *Journal of Computer Science*, *8*(4), 585-590.

Subramanian, A. & Ravi, G. (2011). Voltage collapse enhancement and loss reduction by reactive power. *International Journal of ComputerApplications, 12*(12), 32-42.

Suganyadevia, M. V., & Babulalb, C. K. (2009). Estimating of loadability margin of a power system by comparing Voltage Stability Indices. In *Control, Automation, Communication and Energy Conservation, 2009. INCACEC 2009. 2009 International Conference on* (pp. 1-4). IEEE.

Sunday, O. O. (2009). Power outages in the Nigeria transmission grid. *Research Journal of Applied Sciences*, *4*(1), 1-9.

Taylor, C. W. (1994). *Power System Voltage Stability.* New York: McGraw-Hill.

TCN, (2015). *Daily Operational Report.* Osogbo: Transmission Company of Nigeria (TCN). Unpublished.

Tilwani, M., & Choube, S. C. (2015) Prediction of Voltage Collapse in Power System using Different Indices. International Journal of Science and Research (IJSR). Volume 4 Issue 6, pp1199-1203.

Tiwari, R., Niazi, K. R., & Gupta, V. (2012). Line collapse proximity index for prediction of voltage collapse in power systems. *International Journal of Electrical Power & Energy Systems*, *41*(1), 105-111.

Vadivelu, K. R., & Marutheswar, D. G. (2014). Maximum Load-ability Estimation for Weak Bus Identification Using Fast Voltage Stability Index in a Power Transmission System by Real-Time Approach. *International Journal of Electrical and Electronics Engineering &Telecommunications, ISSN*, 2319-2518: 84-91.

Veleba, J., & Nestorovic, T. (2013). Performance of Static Voltage Stability Analysis in MATLAB Environment with Further Applications. *International journal of education and information technologies, 4*(7).133-145

Verayiah, R., Mohamed, A., Shareef, H., & Abidin, I. H. Z. (2013). Performance comparison of voltage stability indices for weak bus identification in power systems. In *IOP Conference Series: Earth and Environmental Science* (Vol. 16, No. 1) . 012022): 1-4. Available from: http://iopscience.iop.org/article/10.1088/1755-1315/16/1/012022/pdfIOP Publishing: doi:10.1088/1755-1315/16/1/012022

Yahia, E. Z., Elsherif, M. A., & Zaggout, M. N. (2015). Detection of Proximity to Voltage Collapse by Using L–Index. *International Journal of Innovative Research in Science Engineering and Technology*, *4*(3), 1755-1765.

APPENDIX A

PROGRAM FOR POWER FLOW ANALYSIS FOR IEEE 14-BUS TEST SYSTEM

```
% IEEE14 bus Test System
%Program For Load Flow Analysis Using Newton-Raphson Method
clear;              %clears all variables from workspace
basemva=100;
accuracy=0.001;
accel=1.6;          %acceleration factor
maxiter=200;        % maximum number of iteration
method;             % Newton Raphson Method

 %Bus code= 0 for load bus, 1 for slack bus, 2 for voltage
%            controlled bus
%        Bus Bus Voltage Angle   ---Load---- -------Generator----- Static Mvar
%        No code Mag.    Degree MW    Mvar     MW Mvar Qmin Qmax    +Qc/-Ql
busdata=[1   1    1.060   0.0     0       0       0    0     0    0       0
         2   2    1.045   0.0    21.7    12.7    0.0 42.4  -40   50       0
         3   2    1.01    0.0    94.2    19.0     0    0     0   40       0
         4   0    1.0     0.0    47.8   -3.9      0    0     0   0        0
         5   0    1.0     0.0    7.6     1.6      0    0     0   0        0
         6   2    1.0     0.0    11.2    7.5      0    0    -6   24       0
         7   0    1.0     0.0    0       0        0    0     0   0        0
         8   2    1.0     0.0    0       0        0    0    -6   24       0
         9   0    1.0     0.0    29.5 16.6        0    0     0   0        0
         10  0    1.0     0.0    9.0     5.8      0    0     0   0        0
         11  0    1.0     0.0    3.5     1.8      0    0     0   0        0
         12  0    1.0     0.0    6.1     1.6      0    0     0   0        0
         13  0    1.0     0.0    13.5    5.8      0    0     0   0        0
         14  0    1.0     0.0    14.9    5.0      0    0     0   0       0];

%                          Line code
%          Bus bus   R       X      1/2 B    = 1 for lines
%          nl  nr  p.u.    p.u.    p.u.     > 1 or < 1 tr. tap at bus nl
```

```
linedata=[1   2 0.01938 0.05917 0.02640        1
          1   5 0.05403 0.22304 0.02190        1
          2   3 0.04699 0.19797 0.01870        1
          2   4 0.05811 0.17632 0.02460        1
          2   5 0.05695 0.17388 0.01700        1
          3   4 0.06701 0.17103 0.01730        1
          4   5 0.01335 0.04211 0.00640        1
          4   7 0       0.20912 0              1
          4   9 0       0.55618 0              1
          5   6 0       0.25202 0              1
          6  11 0.09498 0.1989  0              1
          6  12 0.12291 0.25581 0              1
          6  13 0.06615 0.13027 0              1
          7   8 0       0.17615 0              1
          7   9 0       0.11001 0              1
          9  10 0.03181 0.0845  0              1
          9  14 0.12711 0.27038 0              1
          10 11 0.08205 0.19207 0              1
          12 13 0.22092 0.19988 0              1
          13 14 0.17093 0.34802 0              1];

lfybus                            % form the bus admittance matrix
if method
else lfnewton              % Load flow solution by Newton Raphson
Method if method
end
busout              % Prints the power flow solution on the screen
lineflow          % Computes and displays the line flow and losses
Lmn_index_1
%Fvsi_index
Fvsi_index_1
%Hybrid_index
Hybrid_index_1
Lqp_index
%
fprintf('\n')
fprintf('               Voltage Collapse Proximity Line Indices \n\n')
```

```
fprintf('       Line     From  To       Lmn       Fvsi       Hsi
Lqp\n')
fprintf('       No.      Bus   Bus           \n')
for k = 1 : nbr
    fprintf('    %5g', k), fprintf('  %5g', nl(k)), fprintf(' %5g',
nr(k)), fprintf('    %7.5f', Lmn(k)), fprintf('    %7.5f', Fvsi(k)),
fprintf('    %7.5f', Hsi(k)), fprintf('    %7.5f\n', Lqp(k))
end
%
%
```

APPENDIX B

PROGRAM FOR POWER FLOW ANALYSIS OF THE NNG 28-BUS TEST SYSTEM

```
%Ph.D work on Voltage Collapse prediction.
%PROGRAM FOR LOAD FLOW ANALYSIS OF THE 28 BUSES OF THE NNG
%USING NEWTON-RAPHSON METHOD
clear;                    %clears all variables from workspace
basemva=100;
accuracy=0.001;
accel=1.6;               %acceleration factor
maxiter=500;             % maximum number of iteration
method=2;                %choose 2 for Newton Raphson Method

%            Bus code=  0 for load bus, 1 for slack bus, 2 for voltage
%            controlled bus
%        Bus Bus  Voltage Angle   ---Load---- -------Generator----- Static
Mvar
%        No  code Mag.    Degree  MW    Mvar         MW  Mvar   Qmin Qmax
+Qc/-Ql
busdata=[1   1    1.050   0.0      0.0    0.0          0      0 -1006 1006     0
         2   2    1.050   0.0     0      0            670    0 -1030 1000     0
         3   0    1.0     0.0    274.4  205.8         0      0    0   0        0
         4   0    1.0     0.0    344.7  258.5         0      0    0   0        0
         5   0    1.0     0.0    633.2  474.9         0      0    0   0        0
         6   0    1.0     0.0    13.8   10.3          0      0    0   0        0
         7   0    1.0     0.0    96.5   72.4          0      0    0   0        0
         8   0    1.0     0.0    383.4  287.5         0      0    0   0        0
         9   0    1.0     0.0    275.8  206.8         0      0    0   0        0
         10  0    1.0     0.0    201.2  150.9         0      0    0   0        0
         11  2    1.05    0.0    52.5   39.4          431.0 0 -1000  1000     0
         12  0    1.0     0.0    427.0  320.2         0      0    0   0        0
         13  0    1.0     0.0    177.9  133.4         0      0    0   0        0
         14  0    1.0     0.0    184.6  138.4         0      0    0   0        0
         15  0    1.0     0.0    114.5  85.9          0      0    0   0        0
         16  0    1.0     0.0    130.6  64.23         0      0    0   0        0
         17  0    1.0     0.0    11     8.2           0      0    0   0        0
         18  2    1.05    0.0    0      0             495    0  -1050 1050     0
```

```
         19  0    1.0     0.0    70.3   52.7          0      0    0   0       0
         20  0    1.0     0.0    193    144.7         0      0    0   0       0
         21  2    1.05    0.0    7.5    5.2           624.7 0  -1010 1010     0
         22  0    1.0     0.0    220.6  142.9         0      0    0   0       0
         23  2    1.05    0.0    70.3   36.1          388.9 0  -1000 1000     0
         24  2    1.05    0.0    20.6   15.4          190.3 0  -1000 1000     0
         25  0    1.0     0.0    110    89.0          0      0    0   0       0
         26  0    1.0     0.0    290.1   145          0      0    0   0       0
         27  2    1.05    0.0    0      0             750    0  -1000 1000     0
         28  2    1.05    0.0    0      0             750    0  -1000 1000   0];

%                                        Line code
%          Bus bus   R       X     1/2 B   = 1 for lines
%          nl  nr  p.u.   p.u.   p.u.     > 1 or < 1 tr. tap at bus nl
linedata=[3   1 0.0006 0.0044 0.029        1
          4   5 0.0007 0.0050 0.0333       1
          1   5 0.0023 0.0176 0.1176       1
          5   8 0.0110 0.0828 0.5500       1
          5   9 0.0054 0.0405 0.2669       1
          5   10 0.0099 0.0745 0.4949      1
          6   8 0.0077 0.0576 0.3830       1
          2   8 0.0043 0.0317 0.2101       1
          2   7 0.0012 0.0089 0.0589       1
          7   24 0.0025 0.0186 0.1237      1
          8   14 0.0054 0.0405 0.2691      1
          8   10 0.0098 0.0742 0.4930      1
          8   24 0.0020 0.0148 0.0982      1
          9   10 0.0045 0.0340 0.2257      1
          15  21 0.0122 0.0916 0.6089      1
          10  17 0.0061 0.0461 0.3064      1
          11  12 0.0010 0.0074 0.0491      1
          12  14 0.0060 0.0455 0.3025      1
          13  14 0.0036 0.0272 0.1807      1
          16  19 0.0118 0.0887 0.5892      1
          17  18 0.0002 0.0020 0.0098      1
          17  23 0.0096 0.0721 0.4793      1
          17  21 0.0032 0.0239 0.1589      1
          19  20 0.0081 0.0609 0.4046      1
          20  22 0.0090 0.0680 0.4516      1
          20  23 0.0038 0.0284 0.1886      1
```

```
        23  26 0.0038 0.0284 0.1886      1
        12  25 0.0071 0.0532 0.3800      1
        19  25 0.0059 0.0443 0.3060      1
        25  27 0.0079 0.0591 0.3900      1
        5   28 0.0016 0.0118 0.0932      1];

lfybus                         % form the bus admittance matrix
if method==1
    lfgauss                % Load flow solution by Gauss-Seidel method
if method=1
else lfnewton              % Load flow solution by Newton Raphson
Method if method
end
busout              % Prints the power flow solution on the screen
lineflow          % Computes and displays the line flow and losses
Lmn_index
Fvsi_index_1
Hybrid_index_NNG28
%
fprintf('\n')
fprintf('               Voltage Collapse Proximity Line Indices \n\n')
fprintf('       Line    From  To      Lmn       Fvsi       Hsi
Lqp\n')
fprintf('       No.     Bus   Bus           \n')
for k = 1 : nbr
    fprintf('    %5g', k), fprintf('  %5g', nl(k)), fprintf(' %5g',
nr(k)), fprintf('    %7.5f', Lmn(k)), fprintf('    %7.5f', Fvsi(k)),
fprintf('    %7.5f', Hsi(k)), fprintf('    %7.5f\n', Lqp(k))
end
```

APPENDIX C
STABILITY INDICES CODE FOR CASE STUDIES

%Stability indices code for case studies

```
% Lmn_index computes the Lmn voltage stability line index

fprintf('\n')
fprintf('    Voltage Collapse Proximity Line Index \n\n')
fprintf('       Line    From  To     Lmn  \n')
fprintf('       No.     Bus   Bus          \n')
del = 0; theta=0; den=0; Lmn=0; Qj=0;
for k = 1 : nbr
    theta(k) = atand(X(k)/R(k));
    del(k) = (deltad(nl(k)) - deltad(nr(k)));
    den(k) = (V(nl(k))*sind(theta(k) - del(k)))^2;
    Qj(k) = imag(Spq(k))/basemva;
    Lmn(k) = abs(4*X(k)*Qj(k)/den(k));
    fprintf('    %5g', k), fprintf('  %5g', nl(k)), fprintf('
%5g', nr(k)), fprintf('    %7.5f\n', Lmn(k))
end
% Fvsi_index computes the FVSI voltage stability index
fprintf('\n')
fprintf('          Voltage Collapse Proximity Line Index \n\n')
fprintf('       Line    From  To     FVSI  \n')
fprintf('       No.     Bus   Bus          \n')
del = 0; theta=0; den=0; Fvsi=0; Qj=0;
for k = 1 : nbr
    denf(k) = V(nl(k))^2*X(k);
    Qj(k) = imag(Spq(k(k>0)))/basemva;
    Fvsi(k) =abs(4*(Z(k)^2)*Qj(k(k>0))/denf(k));
    fprintf('    %5g', k), fprintf('  %5g', nl(k)), fprintf('
%5g', nr(k)), fprintf('    %7.5f\n', Fvsi(k))
end
```

```
% Hybrid line stability index IEEE 14 bus system
fprintf('\n')
fprintf('               Voltage Collapse Proximity Line Index
\n\n')
fprintf('       Line    From  To     Hsi  \n')
fprintf('       No.     Bus   Bus          \n')
del = 0; theta=0; denh=0; Hsi=0; Qj=0; s=0;
for k = 1 : nbr
    Qj(k) = imag(Spq(k))/basemva;
     del(k) = (deltad(nl(k)) - deltad(nr(k)));
     theta(k) = atand(X(k)/R(k));
    if abs(del(k)) >= 1.422,  s = 0; else s = 1; end
        A=4*Qj(k)/abs(V(nl(k)))^2;
        B=abs(Z(k)^2)*s/X(k);
        C=X(k)*(s-1)/sind(theta(k) - del(k))^2;
        Hsi(k)= abs(A*(B-C));

    fprintf('    %5g', k), fprintf('  %5g', nl(k)), fprintf('
%5g', nr(k)), fprintf('    %7.5f\n', Hsi(k))
end
% Hybrid line stability index NNG bus 28
fprintf('\n')
fprintf('               Voltage Collapse Proximity Line Index
\n\n')
fprintf('       Line    From  To     Hsi  \n')
fprintf('       No.     Bus   Bus          \n')
del = 0; theta=0; denh=0; Hsi=0; Qj=0; s=0;
for k = 1 : nbr
    Qj(k) = imag(Spq(k))/basemva;
     del(k) = (deltad(nl(k)) - deltad(nr(k)));
     theta(k) = atand(X(k)/R(k));
    if abs(del(k)) >= 4.076,  s = 0; else s = 1; end
```

```
        A=4*Qj(k)/abs(V(nl(k)))^2;
        B=abs(Z(k)^2)*s/X(k);
        C=X(k)*(s-1)/sind(theta(k) - del(k))^2;
        Hsi(k)= abs(A*(B-C));

    fprintf('    %5g', k), fprintf('  %5g', nl(k)), fprintf('
%5g', nr(k)), fprintf('    %7.5f\n', Hsi(k))
end
```

APPENDIX D

PUBLICATIONS

- **Isaac A. Samuel**, James Katende, Claudius O. A. Awosope and Ayokunle A. Awelewa. “Prediction of Voltage Collapse in Electrical Power System Networks using a New Voltage Stability Index.” International Journal of Applied Engineering Research ISSN 0973-4562 Volume 12, Number 2 (2017) pp. 190-199. http://www.ripublication.com

- **Isaac Samuel**, James Katende, S. Adebayo Daramola and Ayokunle Awelewa “Review of System Collapse Incidences on the 330-kV Nigerian National Grid” International Journal of Engineering Science Invention ISSN (Online): 2319 – 6734, ISSN (Print): 2319 – 6726 Volume 3Issue 4 ǁ April 2014 ǁ PP.55-59.

- **Isaac A. Samuel,** Okwechime Ngozi Marian, and Ademola Abudulkareem “investigating the selection of a suitable slack bus: a case study of the multi-generating stations of the nigerian 330-kv power system network.” International Journal of Electrical Electronic Engineering Studies Vol.2, No.1, pp.1-12, September 2014.

- **Isaac Samuel**, James Katende and Frank Ibikunle “Voltage Collapse and the Nigerian National Grid.” Presented at the EIE 2nd International Conference on Computing, Energy, Networking, Robotics and Control and Telecommunications. November, 21st – 23rd 2012 (Presented Paper)